EYE VERSUS HAND EFFECTOR-SPECIFICITY IN THE PARIETO-FRONTAL CORTEX AND CEREBELLUM IN HUMANS

KIANA MASOUDI

A THESIS SUBMITTED TO THE FACULTY OF GRADUATE STUDIES IN PARTIAL FUFILLMENT OF THE REQUIREMENTS FOR A MASTER OF SCIENCE DEGREE

MASTER OF SCIENCE PROGRAM IN KINESIOLOGY AND HEALTH SCIENCES

YORK UNIVERSITY

TORONTO, ONTARIO, CANADA

JULY 2026

© Kiana Masoudi, 2026

ABSTRACT

The degree and distribution of effector-specific representations for saccade and reach movements in the human brain remains unclear, partly because the low temporal resolution of fMRI blurs sensorimotor phases. Using an event-related paradigm, we examined brain activity across (1) *visual target encoding*, (2) *movement planning*, and (3) *movement execution* phases in 19 adults. Target encoding activated temporal and frontal regions while saccade planning recruited posterior parietal regions and reach planning produced broad occipital-parietal-frontal activity. During execution, both cortical networks were engaged. Conjunction analyses revealed overlapping activity confined to saccade areas. Effector-specific differences were clear during execution, with saccade-preferential activity in frontal and lateral posterior parietal regions and reach-preferential activity in sensorimotor and medial posterior parietal areas, as well as the ipsilateral cerebellum. Region-of-interest (ROI) analyses revealed greater activity for reach, except in right primary visual cortex (V1) and left midposterior intraparietal sulcus (mIPS). These findings confirm that separating sensorimotor phases improves the detection of effector-preferential signals across the brain.

ACKNOWLEDGEMENTS

I would like to thank Dr. J. Douglas Crawford for his mentorship and support throughout my entire Master's. From him, I've learned how to navigate the complexities of science with patience and thoughtfulness.

I am also deeply grateful to Dr. Cristina Rubino for teaching me everything there is to know about creating and conducting a neuroimaging study. Witnessing her dedication throughout the past two years has taught me what it truly means to be a scientist. It is no exaggeration to say this work would not have been possible without her.

I would also like to thank all past and current lab members of the Crawford Lab for welcoming me and helping me at every step of the way, especially John Lio for his assistance with data collection.

I am especially grateful for the help of Dr. Diana Gorbet and Chi Cheng for their help with this entire experiment.

I would like to also thank my committee members, Dr. Lauren Sergio and Dr. Denise Henriques, for their valuable feedback and support.

Thank you as well to all of the friends I have made along the way.

Finally, the biggest thanks go to my parents and sister for everything they have done for me, the list of which could easily fill up this entire thesis.

TABLE OF CONTENTS

ABSTRACT ii

ACKNOWLEDGEMENTS iii

TABLE OF CONTENTS iv

LIST OF TABLES vi

LIST OF FIGURES vii

CHAPTER 1: INTRODUCTION 1

1.1 The Saccade System 2

1.1.1 Animal Neurophysiology 2

1.1.2 Human Experiments: Functional Neuroimaging, Lesions and Brain Stimulation 4

Animal Neurophysiology 7

Human Reach System: Neuroimaging, Lesions and Stimulation 8

1.3 Eye vs. Hand: Overlap and Effector Specificity in the Human Cortex 10

1.4 Gap in Literature 12

1.5 Research Questions 13

1.6 Hypotheses 14

CHAPTER 2: METHODS 16

2.1 Participants 16

2.2 Experimental Apparatus 16

2.4 Training and Behavioural Recordings 20

2.5 Imaging Parameters 21

2.6 Preprocessing 22

2.7 Data Analysis 22

2.7.1 Behavioural Analysis and Exclusion Criteria 22

2.7.2 Univariate Analysis 23

2.7.3 Conjunction Analysis 25

2.7.4 Region of Interest Analysis 25

2.7.5 Statistical Analysis 26

CHAPTER 3: RESULTS 28

3.1 Effector versus colour activation across encoding, planning, and execution 28

3.1.1 Visual Target Encoding 29

3.1.2 Movement Planning 30

3.1.3 Movement Execution 32

3.2 Overlapping saccade and reach activation during planning and execution 36
3.2.1 Movement Planning 36
3.2.2 Movement Execution 37
3.3 Effector-preferential activation across planning and execution 39
3.3.1 Movement planning 40
3.3.2 Movement Execution 43
3.4 Region-of-interest analysis 47
3.4.1 Movement Planning 47
3.4.2 Movement Execution 48
CHAPTER 4: DISCUSSION 50
4.1 Effector versus colour activation across encoding, planning, and execution 51
4.1.1 Visual Target Encoding 51
4.1.2 Movement Planning 51
4.1.3 Movement Execution 52
4.2 Overlapping Saccade and Reach activation 53
4.3 Effector-preferential activation across planning and execution 54
4.3.1 Movement Planning 54
4.3.2 Movement Execution 55
4.4 Limitations 56
4.5 Future Directions and Potential Applications 58
4.6 Conclusion 58
REFERENCES 60
APPENDIX 71

LIST OF TABLES

Table 1: ROI Analysis Information.....26

Table 2: List of brain region abbreviations.....28

Table 3: Cluster information for the visual target encoding.....30

Table 4: Cluster information for saccade and reach planning.....32

Table 5: Cluster information for saccade and reach execution.....36

Table 6: Cluster information for saccade- and reach-preferential planning 44

Table 7: Cluster information for saccade- and reach-preferential execution.....47

LIST OF FIGURES

Figure 1: Overview of cortical and subcortical regions involved in saccade control.....3

Figure 2: 'Flattened' anatomical representation of the cerebellum.....4

Figure 3: Overview of cortical regions involved in saccade and reach control.....6

Figure 4: Overview of monkey PPC regions involved in reach and saccade control.....8

Figure 5: Overview of human PPC regions involved in reach and saccade control.....10

Figure 6: Summary of reported overlap in PPC regions for reach and saccade control.....12

Figure 7: Image of the experimental set-up.....17

Figure 8: Illustration of the experimental paradigm.....20

Figure 9: Cortical statistical map for visual target encoding.....30

Figure 10: Cortical statistical maps for the saccade and reach planning.....32

Figure 11: Cortical statistical maps for the saccade and reach execution.....34

Figure 12: Cerebellar statistical maps for the saccade and reach execution.....35

Figure 13: Cortical saccade and reach planning conjunction map.....38

Figure 14: Cortical saccade and reach execution conjunction map.....39

Figure 15: Cerebellar saccade and reach execution conjunction map.....40

Figure 16: Cortical statistical maps for saccade- and reach-preferential planning.....42

Figure 17: Cerebellar statistical maps for saccade- and reach-preferential planning.....43

Figure 18: Cortical statistical maps for saccade and reach-preferential execution.....45

Figure 19: Cerebellar statistical maps for saccade and reach-preferential execution.....46

Figure 20: ROI analysis for saccade versus reach planning.....49

Figure 21: ROI analysis for saccade versus reach execution.....50

CHAPTER 1: INTRODUCTION

Humans rely on eye and arm movements to interact with the world around them. These movements require sensory information, such as visual and proprioceptive cues, which posterior parietal and frontal regions process and integrate to generate appropriate action plans. Brain signals are eventually transformed into muscle commands that travel via the peripheral nervous system to control the movement of the eyes and hands (Kalaska & Crammond, 1992; Vingerhoets, 2014).

A series of non-human primate and human studies have extensively examined the neural regions involved in controlling eyes and arm movements, in particular, visually-guided saccades and reaches. Saccades describe rapid eye movements that bring visual information into fixation (Rayner, 1998), while reaches are defined as the transportation of the arm and hand towards a target (Filimon et al., 2009; Vesia & Crawford, 2012). In non-human primates, distinct signals related to saccades and reaches have been identified along the posterior parietal cortex (PPC) and frontal regions (Bruce & Goldberg, 1985; Barash et al. 1991; Johnson et al., 1996; Snyder et al., 1997; Andersen & Buneo, 2002). Conversely, in humans, separating saccade- and reach-specific signals has proven to be more challenging, although homological regions have been specified to some extent (Vesia & Crawford, 2012). Still, most functional magnetic resonance imaging (fMRI) studies report substantial overlap between the neural regions recruited for these effectors (Astafiev et al., 2003; Levy et al., 2007; Beurze et al., 2009; Filimon et al., 2009). Many factors can contribute to the difficulty in dissociating reach and saccade signals, including the relatively low spatial resolution of fMRI and the fact that eye and hand movements are typically tightly coupled in everyday tasks, which suggests that there might actually be a shared network for these effectors (Levy et al., 2007; Gallivan et al., 2011). Considering all these factors, to date, the degree of effector specialization remains unclear. Consequently, a central question in sensorimotor neuroscience is: to what degree does the brain exhibit effector-specific activations for saccades and reaches? Addressing this question will provide a framework for understanding the neural representations of different goal-directed movements.

1.1 The Saccade System

1.1.1 Animal Neurophysiology

Electrophysiology studies in non-human primate have identified regions and pathways involved in the control of saccades, summarized in **Figure 1**. In the visual cortex, neurons in area V3A encode visual stimulus location in a gaze-dependent manner, meaning the same retinal input evokes different neuron responses based on gaze direction (Galletti & Battaglini, 1989). Visual information from V3A is then relayed to the PPC, where a relative functional organization has been proposed, with eye movements preferentially engaging more lateral regions of the intraparietal sulcus (IPS) and reaches engaging more dorsal and medial areas (Vesia and Crawford, 2012). V3A neurons particularly project to the lateral bank of the intraparietal sulcus (LIP), which is involved in saccade planning (Blatt et al., 1990). LIP neurons show activity during visual target presentation as well as preparation and execution of saccades (Barash et al. 1991). Neurons from this area project to both the frontal eye field (FEF) and superior colliculus (SC), positioning it as a critical region between visual processing and saccade generation (Ferraina et al. 2002).

The FEF, located in the frontal cortex, is involved in the generation and selection of saccades. Different subpopulations of FEF neurons are active during the preparation and execution of saccades (Bruce and Goldberg, 1985). Since multiple stimuli can often compete for a saccadic response, the FEF is also involved in determining the correct saccade target. Schall and Hanes (1993) demonstrated that FEF neurons initially respond equally to a target and distractors, but this activity evolves to select target location prior to saccade execution. Near the supplementary motor area (SMA), the supplementary eye field (SEF) also contributes to saccade preparation, and micro-stimulation of this region can evoke saccades (Schlag & Schlag-Rey, 1987).

More anteriorly, the dorsolateral prefrontal cortex (DLPFC) supports higher-order cognitive processes involved in saccade control. DLPFC neurons show sustained activity during the delay period of memory-guided saccades, with neurons responding preferentially to specific

spatial locations of remembered cues. This suggests that the DLPFC helps maintain spatial information in the working memory to guide accurate saccades (Funahashi et al., 1989).

Within the subcortex, the caudate nucleus of the basal ganglia receives inputs from FEF and plays a role in saccade control (Stanton et al., 1988). Prior to a saccade, the CD suppresses the inhibitory output of the substantia nigra pars reticulata (SNr), which in turn disinhibits the SC and allows saccade initiation (Hikosaka et al., 1993). The SC is central to saccade generation, with stimulation of its neurons evoking saccades whose direction and amplitude depend on the stimulation site, indicating a topographic map of saccade vectors (Robinson et al., 1972). SC neurons then project to saccade-related brainstem premotor circuits to execute eye movements (Wang et al., 2013).

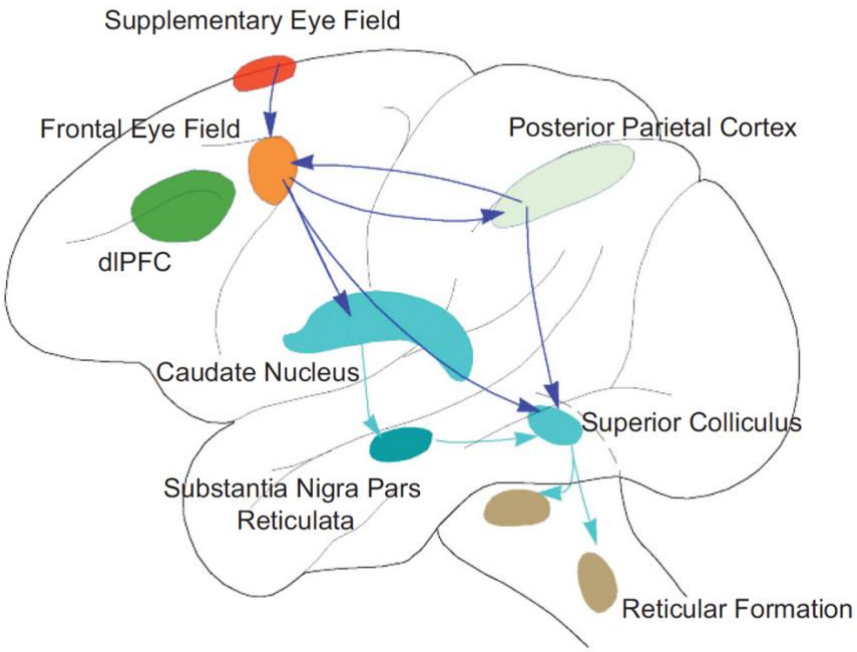


Figure 1: Overview of cortical and subcortical regions involved in saccade control. Figure reproduced from Pouget (2015).

The cerebellum, particularly the oculomotor vermis (OMV; lobules VI-VII), receives projections indirectly from FEF through nucleus reticularis tegmenti pontis (NRTP) to support the online control of saccades (Künzle and Akert, 1977; Brodal, 1980). **Figure 2**

provides an illustration of 'flattened' cerebellum, including the posterior vermis, where OMV resides. Stimulation of this region evokes saccade-like movements (Fujikado & Noda, 1987). The OMV projects via Purkinje cells to the fastigial oculomotor region (FOR) to refine saccade metrics, such as amplitude and termination. The FOR then modulates brainstem generators, including the paramedian pontine reticular formation (PPRF) and SC, to regulate saccade initiation, trajectory, and termination (Noda et al., 1990; Ohtsuka & Noda, 1991).

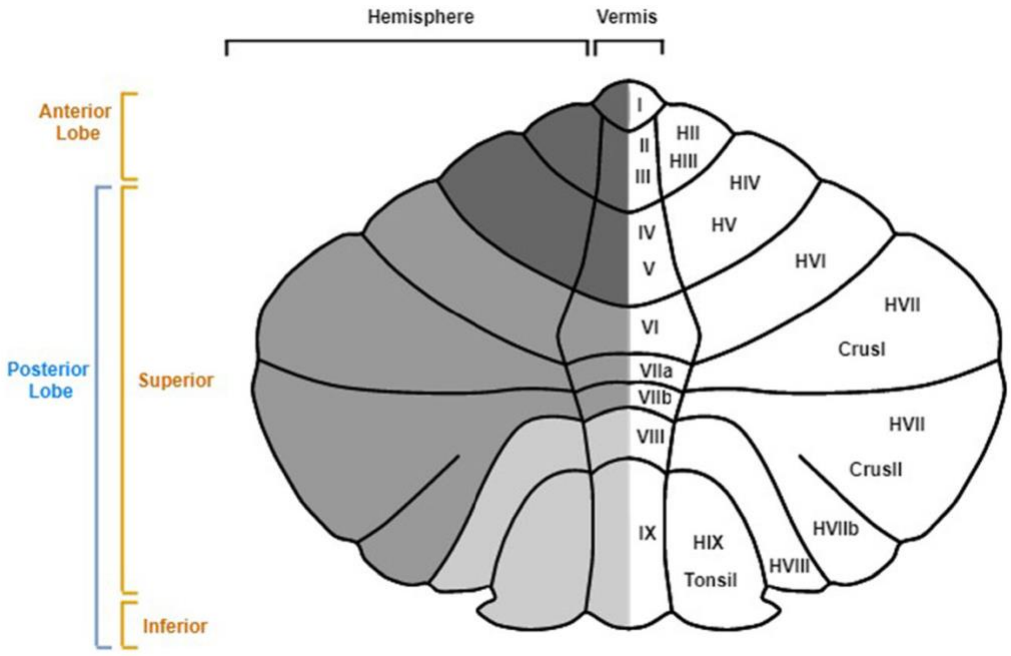


Figure 2: 'Flattened' anatomical representation of the cerebellum, showing the anterior and posterior lobes, as well as hemispheric and vermal subdivisions. Figure reproduced from Fernandez et al. (2020).

1.1.2 Human Experiments: Functional Neuroimaging, Lesions and Brain Stimulation

Figure 3 provides the hypothetical flow of information for saccade processing across the human brain (in red). fMRI studies indicate that saccades recruit parieto-frontal areas that largely overlap with the reach network, although many regions show lower magnitudes of activation for saccades compared to reaches (Astafiev et al., 2003; Filimon et al., 2009).

Visual information is relayed from occipital regions to the PPC, where several regions have been implicated in saccade processing. Transcranial magnetic stimulation (TMS) to the PPC delays saccade initiation, with distinct effects for the left and right hemispheres (Kapoula et al., 2005). Within this region, an anterior-posterior gradient for saccade versus reach processing has been proposed, with posterior regions showing stronger visual- and saccade-related responses, intermediate regions demonstrating reach- and saccade-activity, and anterior areas showing stronger activation for reaching (Levy et al., 2007; Filimon et al., 2009). Along the medial-lateral axis, saccadic activity preferentially recruits more lateral regions of the IPS, whereas reaches show preferential activity more medially (Levy et al., 2007). Supporting this functional dissociation, bilateral lesions restricted to the medial IPS impair visually-guided reaching while saccadic movement remain largely normal (Trillenberg et al., 2007).

At the regional level, the midposterior IPS (mIPS) contribute to the planning of eye movements towards a spatial goal (Astafiev et al., 2003; Filimon et al., 2009). Saccadic-related activity has also been observed in the supramarginal gyrus (SMG; Simo et al., 2005; Yamamoto et al., 2025), angular gyrus (AG; Simo et al. 2005; Schraa-Tam, 2009), inferior parietal lobule (IPL; Yamamoto et al., 2025), precuneus (Simo et al., 2005), superior parietal lobe (SPL; Koyama et al., 2004; Filimon et al., 2009), and parietooccipital sulcus (POS; Beurze et al., 2009). TMS applied to the right mIPS and right AG during saccade planning reduces the accuracy of contralateral saccades (Vesia et al. 2010).

Information from PPC, particularly the SPL and IPS, is relayed to the frontal cortex, projecting to the FEF, and maintaining bidirectional connections with DLPFC and the premotor cortex (Rolls et al., 2023). The frontal eye field (FEF) within the precentral sulcus is involved in the preparation and generation of saccadic eye movements (Medendorp et al. 2005; Filimon et al., 2009; Gallivan et al., 2011; Pouget, 2015). TMS delivered to this region delays memory-guided saccade initiation (Yang & Kapoula, 2011). Other frontal regions contributing to saccade control include the SEF, located along the medial surface of the superior frontal gyrus (Koyama et al., 2004; Yamamoto et al., 2025), the cingulate motor area (CMA; Pouget,

2015; Beurze et al., 2009), and prefrontal cortex (Simo et al., 2005). Additionally, the DLPFC, plays a role in the executive control of saccades, with TMS stimulation of this site impairing anti-saccade performance (Cameron et al., 2015).

Within the cerebellum, the posterior vermis (VI-VII) and adjacent hemispheres are activated for reflexive, voluntary, and memory-guided saccades (Miall et al., 2000; Nitschke et al., 2004; Simo et al., 2005; Schraa-Tam et al., 2009; Yamamoto et al., 2025). It has been proposed that vermal activity reflects oculomotor control whereas hemispheric involvement reflects the higher cognitive and spatial working memory demands of certain saccade tasks. Consistent with this, memory-guided saccades reportedly recruited the hemispheric VI-Crus I and VIIb-VIII (Nitschke et al., 2004). Simo et al. (2005) further demonstrated that hemispheric VI-Crus I is significantly more active for predictive (memory-driven) than visually-guided (sensory-driven) saccades. Despite this, patients with cerebellar degeneration show greater impairments in visually-guided than memory-guided saccades, although their findings pertained to the entire cerebellum (Inomata-Terada et al., 2023).

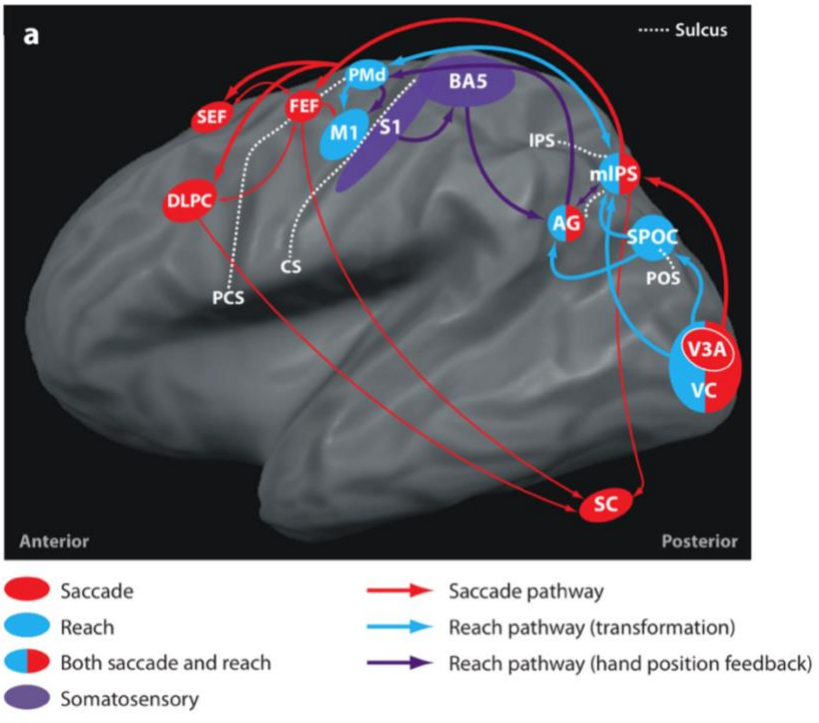


Figure 3: Overview of key cortical regions implicated in saccade (red) and reach (blue) networks. Figure reproduced from Crawford et al., (2011).

1.2 The Reach System

Animal Neurophysiology

Neurophysiological studies on non-human primates have identified numerous PPC areas involved in reaching. A summary of these regions, as well as those indicated for saccade and grasp, are presented in **Figure 4**. Neurons within the medial bank of the IPS (MIP; Johnson et al., 1996; Snyder et al., 1997), V6A, located in the posterior part of the SPL, and the parietal reach region (PRR), an area overlapping MIP and V6A, respond before the onset of and during arm movements (Galletti et al., 1997; Batista et al., 1999). The PRR encodes reach targets in an eye-centered reference frame during reach planning, suggesting that reach goals are first defined in gaze-dependent coordinates before they are transformed into limb-motor commands (Batista et al., 1999).

MIP neurons are connected to frontal premotor and motor regions, specifically the dorsal premotor cortex (PMd; Johnson et al., 1996) and the primary motor cortex (M1; Bakola et al., 2017). The PMd has been established in specifying, planning, and executing reaching movements, with many neurons exhibiting direction-specific tuning for upcoming reach targets (Weinrich and Wise, 1982; Caminiti et al., 1991). Finally, neurons within M1 produce signals that drive the muscle via the peripheral nervous system, although many neurons within this region also encode higher-level movement parameters such as reach direction (Kakei et al., 1999).

The cerebellum contributes to reach control through closed-loop connections with cortical motor areas. Purkinje cells in the cerebellar lobules IV-VI and VIIb to VIII indirectly project to M1 through the dorsal dentate nucleus and ventrolateral thalamus, while the ventral dentate projects to the PPC (Hoover and Strick, 1999; Kelley and Strick, 2003; Dum and Strick, 2003). Functionally, Purkinje cells in ipsilateral lobules V-VI are directionally tuned to arm movements and exhibit simple spike activity that encodes reach kinematics such as direction and distance (Fu et al., 1997). Their activity also precedes movement onset and signals both predictive and feedback-related errors, likely generating sensory prediction errors (Popa et al., 2012). During adaptation to mechanical perturbations, Purkinje cells

encode changes over time, consistent with the cerebellum functioning as a forward internal model for reach control (Hewitt et al. 2015).

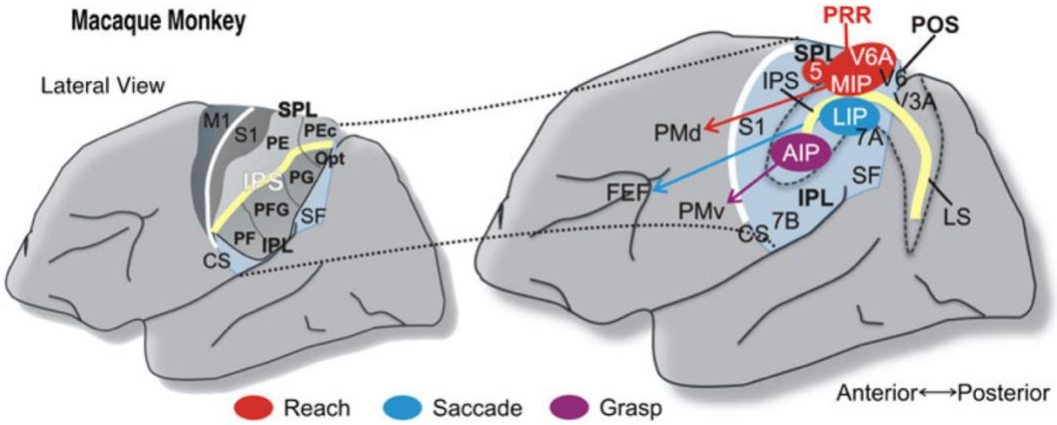


Figure 4: Overview of PPC regions implicated in reach, saccade, and grasp control in monkeys. Figure reproduced from Versia and Crawford (2012).

Human Reach System: Neuroimaging, Lesions and Stimulation

The cortical flow of information for reaches is shown in **Figure 3** (in blue). Visual information is relayed from occipital areas to the PPC, shown in **Figure 5**, for visually-guided reaching. Patients with lesions to this region suffer from optic ataxia, which prevents them from accurately reaching towards peripheral targets in the contralateral visual field, especially with the contralateral hand (Perenin & Vighetto, 1988). Consistent with this, patients with optic ataxia following PPC lesions show impaired integration of proprioceptive hand-position information during reaching (Blangero et al., 2007). Moreover, TMS stimulation of the dorsal-lateral PPC demonstrates its role in integrating hand position to compute a reach vector (i.e., the direction and distance the hand must travel to reach the target; Vesia et al., 2008).

Visual information about the spatial target is processed in a region located near the parieto-occipital junction (POJ), known as the superior parieto-occipital cortex (SPOC). SPOC, sometimes referred to as the homologue of the macaque parietal reach region (PRR), forms internal representations of the spatial goal of arm movements towards contralateral peripheral locations during reach planning (Connolly et al., 2003; Fernandez-Ruiz et al.,

2007), with its activity more visual-driven (Filimon et al., 2009). SPOC is reach-specific, with TMS stimulation impacting reach but not saccade accuracy (Vesia et al., 2010).

Reach planning additionally recruits the mIPS, which integrates target visuospatial information to form reach plans (Beurze et al., 2007; Filimon et al., 2009; Vesia & Crawford, 2012; Cappadocia et al., 2017). TMS stimulation of this region impacts reach-end point variability of the contralateral hand and suggests that mIPS likely uses visual signals about hand position to calculate a reach vector (Vesia et al., 2010). The pIPS is also involved in reach, playing a role in integrating target and effector information to form a movement plan (Beurze et al., 2007; Cappadocia et al., 2017).

Proprioceptive information about hand position is processed in the AG as well as the anterior part of the precuneus (aPCu) along the medial parietal wall. AG shows activation fixed to the extrinsic movement direction while aPCu is active during both visual and non-visual reaching (Fernandez-Ruiz et al., 2007; Filimon et al., 2009; Vesia & Crawford, 2012). Similar to mIPS, TMS stimulation of AG impacts reach end-point variability, suggesting that this region integrates proprioceptive information to calculate a reach vector (Vesia et al., 2008; Fernandez-Ruiz et al., 2007). The SMG also shows activity during reach and may contribute to the cognitive aspects of movement, such as spatial attention and goal representation (Gertz and Fiehler, 2015; Cappadocia et al., 2017).

Reach processing is relayed to frontal regions, such as PMd, which support arm-target integration to form movement goals (Beurze et al., 2007; Gertz and Fiehler, 2015; Cappadocia et al., 2017). Notably, the adjacent FEF is also active, implicating this region in encoding spatial location in an effector-independent manner, aside from its role in eye-movement commands (Astafiev et al., 2003). The ventral premotor cortex (PMv) is also involved in reach control (Beurze et al., 2007; 2009), although this region is mostly involved in grasping and manipulating objects (Chouinard & Pause, 2006; Vesia & Crawford, 2012). Along the medial frontal wall, reaching activates the CMA and SMA, which play roles in movement preparation (Beurze et al., 2007; Filimon et al., 2009; Cappadocia et al.,

2017). Finally, during reach execution, M1 becomes activated, contralateral to the reaching hand (Medendorp et al., 2005; Cappadocia et al., 2017).

Within the cerebellum, upper limb movements are localized in hemispheric and vermal V, with extensions into adjacent regions (lobules IV and VI), and an additional secondary representation in lobule VIII. Activity is predominantly ipsilateral (Grodd et al., 2001). Accordingly, studies have found reach-related activity across the ipsilateral hemispheric lobules IV-VI, Crus I, and VIIb-VIII as well as vermal lobules IV-VII (Nitschke et al., 2004). Cerebellar activity within lobules IV-VI, and VIII has also been linked to target and execution errors during reaching (Diedrichsen et al., 2005) and reach-to-grasp manipulative actions (Errante & Fogassi, 2020). The cerebellum also plays a role in predicting the sensory consequence of reaching movements as patients with cerebellar ataxia show impairments in these predictive processes (Izawa et al., 2012).

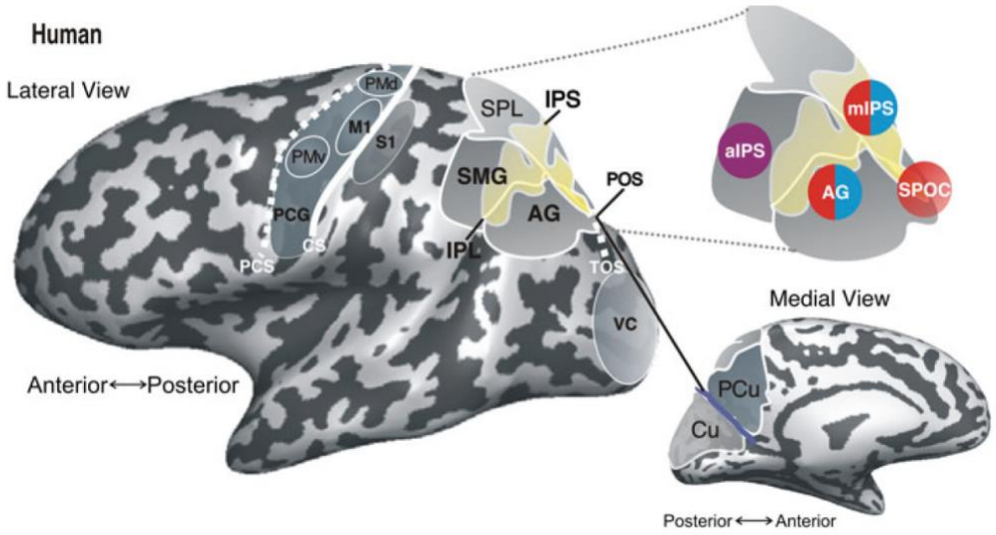


Figure 5: Overview of PPC regions implicated in reach (red), saccade (blue), and grasp (purple) control in humans. Figure reproduced from Versia and Crawford (2012).

1.3 Eye vs. Hand: Overlap and Effector Specificity in the Human Cortex

Along the parieto-frontal cortex, many of the same regions are significantly activated for both reach and saccade tasks (Astafiev et al., 2003; Levy et al., 2007; Beurze et al., 2009; Filimon

et al., 2009). **Figure 6** provides insight into the studies that have implicated the same regions for saccades and reaches within the PPC. Conjunction analyses of saccade and reach planning reveal overlapping activation in bilateral SMA, CMA, PMd, PMv, caudal IPS, anterior IPS (aIPS), and the parieto-occipital sulcus (PO; Beurze et al., 2009). Preliminary findings from Cappadocia et al., (2018) expand on this by showing overlap in left mIPS and right AG, PCu, SPOC, LOTC, FEF/PMv during movement execution. ROI-based analyses also show no significant differences in reach- and saccade- related voxel counts within bilateral IPS1 and FEF during execution (Levy et al., 2007).

Despite the substantial overlap, comparisons between reach and saccade activity reveal effector-dependent differences. While not many studies have explored effector-specific signals using direct contrasts, those that have demonstrate reach-preferential activity during movement planning. Within the left hemisphere, this includes parietal areas (IPL, aIPS, SPL, PCu, AG, SMG), the dorsal precentral gyrus, and anterior cingulate (Astafiev et al., 2003; Cappadocia et al., 2018). Bilateral reach-preferential activity has also been identified in middle occipital gyrus (MOG), mIPS, M1, S1, PMd, and BA24 (Cappadocia et al., 2018). Voxel-level reach preference, pooled across hemispheres, is reported in the SMA, CMA, PMd, M1, cIPS, and aIPS, and POS (Beurze et al., 2009).

During movement execution, reach-preferential activity is observed across a broad parieto-frontal network. Bilateral preference has been reported in mIPS, SMG, S1, M1, PMd, and SMA, while left-lateralized responses are found in lateral occipital cortex (LOC), aIPS, IPL, FEF, SMA, anterior PCu, superior frontal gyrus, and BA24 (Astafiev et al., 2003; Hagler et al., 2007; Levy et al., 2007; Filimon et al., 2009; Cappadocia et al., 2018). In contrast, saccades show preferential activity in visual areas, including the bilateral occipital pole and left V7, as well as the bilateral inferior central sulcus and right FEF (Levy et al., 2007; Filimon et al., 2009; Cappadocia et al., 2018).

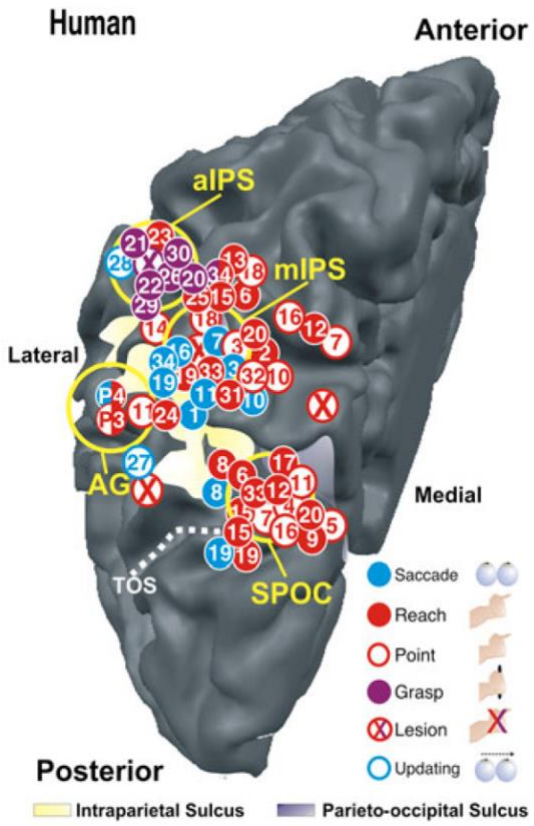


Figure 6: Summary of PPC regions implicated in saccade and reach processing, illustrating the overlap of regions reported for these effectors in fMRI, patient and Transcranial magnetic stimulation (TMS) studies. Numbered markers indicate sites reported across individual studies (A). Proposed homologies between non-human primate and human PPC regions (B). Figure reproduced from (Vesia and Crawford, 2012).

1.4 Gap in Literature

Despite the evidence for cortical overlap and effector-specific differences for saccade and reach processing, findings across studies remain difficult to reconcile. One possible explanation for confounding results is the low temporal resolution of fMRI, which typically images the brain based on a repetition time (TR) in the order of seconds. Consequently, signals associated with different brain regions or temporal events that occur close in time might "blur" together. This temporal conflation may reduce the detection of activity involved in preparing and executing saccades or reaches (Cappadocia et al., 2017). Currently, much of the literature employs task designs that do not separate the three distinct phases involved in performing visually guided movements: (1) perceiving a peripheral target, (2) planning a

movement towards its remembered location, (3) executing that movement. Studies that present a target and instruct an effector (i.e., hand or eyes) in one phase might produce results that reflect both visual target encoding and motor planning. Moreover, those that do not separate planning and execution phases may show effector-independent activation for brain regions that might be involved in both reaches and saccades at different times (Cappadocia et al., 2017).

As cited, the preliminary study by Cappadocia et al. (2018) investigated effector-specificity while addressing this limitation by employing a cue-separation event-related fMRI paradigm that effectively separates visually-guided reaches and saccades into three separate phases: an effector-independent target visual encoding phase, an effector-dependent motor planning phase, and an effector-dependent motor execution phase. This approach revealed distinct temporal progression of sensorimotor processes along the cortex and medial-lateral distinction in effector preference.

While such approaches have advanced our understanding of cortical organizations, it remains unclear whether the same principles expand beyond the cortex. In particular, few fMRI studies have examined cerebellar activation overlaps and differences between saccades and reaches, and they typically focus on separate task contrasts and qualitative comparison of the resulting activity rather than more direct approaches within the same experimental paradigm (Miall et al., 2000; Nitschke et al., 2005). Thus, effector-specific activity within the cerebellum also remains largely unresolved.

1.5 Research Questions

Building on previous work, the present study aimed to employ a cue-separation fMRI paradigm (Cappadocia et al., 2018) to better understand effector-dependent activation across temporal phases of sensorimotor control within both cortical and cerebellar regions. The following questions will be answered:

1. How is functional activity within the saccade and reach network characterized across temporally separated *visual target encoding* as well as *movement planning* and *execution* phases?

2. Which brain regions characterized for saccades and reaches overlap during *movement planning* and *execution* phases?

3. Which brain regions are preferentially activated for saccade versus reach and vice versa during *movement planning* and *execution*?

These questions will be answered both in terms of the *distributions* of activations (i.e., using a whole brain voxel-wise analysis) and *degree* of activation in specific known saccade and reach areas (i.e. through an ROI analysis).

1.6 Hypotheses

Based on previous literature and the findings of Cappadocia et al., (2018), the following hypotheses are formed:

1. There will be shared, effector-independent cortical activity during *visual target encoding*, with saccade- and reach-related cortical (parieto-frontal) and cerebellar signals emerging during the effector-dependent *movement planning* and *execution* phases, with reach planning and execution showing broader activity, lateralized to the left hemisphere (i.e., contralateral to the reaching hand).

2. Overlapping activation between reach and saccade conditions will be observed across key cortical (parieto-frontal) and cerebellar areas that have been implicated for both effectors, with greater overlap during the *movement execution* phase.

3. During *movement planning*, reach-preferential cortical (parieto-frontal) activity will be more widespread compared to saccades. During *movement execution*, there will be a relative medial/lateral separation for reach/saccade activation, respectively, with reach-preferential activity more left-lateralized compared to saccades. Within the cerebellum, saccade-preferential activity will be seen in more medial regions

(i.e., oculomotor vermis) while reach-preferential activity will be ipsilateral to the reaching arm and present across representative hemispheres.

CHAPTER 2: METHODS

2.1 Participants

Twenty, right-handed, healthy adults, with normal or corrected-to-normal vision were recruited from local communities, predominantly from York University. An a priori power analysis was conducted using effect magnitudes in similar visuomotor studies, which observed approximately 0.5% to 1.5% blood-oxygen-level-dependent (BOLD) signal change in pertinent regions of interest across the cortex (Gallivan et al. 2011; Cappadocia et al. 2017). Assuming a large effect size (Cohen's d = 0.8-1.00), $\alpha = 0.05$, and power $(1-\beta) = 0.80$, the analysis indicated 10 to 15 participants would be sufficient to detect expected effects. To account for exclusion of participants due to potential motion artifacts or behavioural errors, an additional five participants were recruited, resulting in the final sample of 20. The York University Human Participants Review Sub-committee approved all methods used in the study. All participants provided informed, written consent prior to the start of the experiment.

2.2 Experimental Apparatus

The experimental apparatus of the present study, shown in **Figure 7**, was similar to Chen et al. (2014) and Cappadocia et al. (2017). Visual stimuli consisted of light emitting diodes (LEDs) that were projected onto a custom-built screen board via fixed optic fibers. A translucent touch screen (Keytec, 170 x 126 mm) was attached to the top of the screen to record touch responses. The screen was fixed to a custom-built platform that was placed over the participant's abdomen in the MRI, with its exact distance adjusted to ensure comfortable reaching. An SR Research EyeLink 1000 Plus eye-tracker was attached to the MRI bed using an adjustable holder, to the side and behind the platform. The exact position of the camera was modified for clear viewing of the participant's left eye. Additionally, five independent custom-built illuminators were attached to the platform using adjustable holders, positioned above the screen to illuminate the eye.

The participant's head was tilted ~20° to allow for a comfortable view of the screen. The left arm rested alongside the body while the right arm was bent to allow the hand to rest on a

button box placed on the abdomen. This marked the 'home' or 'starting' position. Participants wore MRI-compatible headphones to hear task-related instructions and communicate with researchers between experimental runs. Throughout the entire imaging session, the MRI room was completely dark, with the only light coming from the LEDs on the touch screen and the eye-tracking illuminators. As such, participants were not able to see their hand during trials, up until the movement execution phase, at which point it was possibly visible as the hand got closer to the screen.

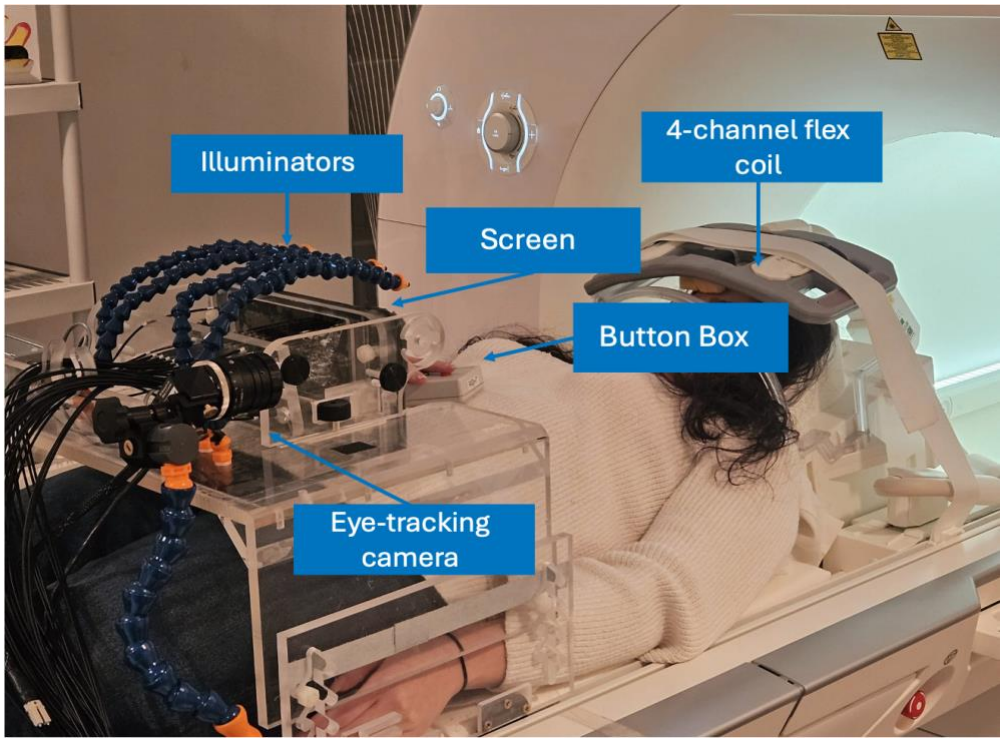


Figure 7: Image of the experimental set-up. Participants performed the experimental tasks in the MRI bore by interacting with a screen positioned above their torso. A button box placed on their abdomen was used for the right hand's 'home' or 'starting' position and for responses during the control task. Left eye-movements were recorded using an eye-tracking camera, with five illuminators mounted above the screen to provide illumination for the eye.

2.3 Experimental Paradigm

An event-related design was used, with the paradigm including three tasks: saccade ("look"), reach ("reach"), as well as colour-report ("colour"), which served as the control. Participants completed these tasks with the support of visual stimuli presented on the screen. These consisted of one yellow central fixation dot and red or green peripheral targets that were presented 4-7° left or right of the midline, on the same horizontal plane. In addition, twenty white "mask" LEDs were presented during delay phases of each trial, with ten appearing on each side of the midline, five below and five above the horizontal target line. These masks were used to control for visual after images of the visual targets and encouraged participants to focus on remembered stimuli (Sereno et al. 2001; Medendorp et al. 2003). All visual stimuli had a diameter of 3mm. Information regarding the stage at which these visual stimuli appeared within a trial is outlined in the following section.

Figure 8 illustrates the sequence of events in each trial. Each run of trials began with 12 seconds of central fixation before the start of the first trial to help stabilize the BOLD signal. Subsequent trials were cued with the flashing of the central yellow LED at the end of a preceding trial. Participants were instructed to keep their hand and eyes at the 'home' position (i.e., their right hand on the button box and eyes fixating the central yellow LED) through the entire trial until the *movement execution* phase. During the first 1.2 seconds, participants were told if this was a "move" or "colour" trial. A red or green peripheral target then appeared either on the left or right side of the yellow LED. Following this, the *visual target encoding* phase began, with white mask LEDs presented for 6 seconds while participants continued fixating. During the 1.2 second period after the mask disappeared, an auditory instruction indicated either "reach", "look", or "colour" (initiating the effector-dependent planning phase). This was followed by the second 6-second delay period, corresponding to the *movement planning* phase, during which time the white LED masks reappeared. Following this, participants heard a "beep" sound, which served as the go-signal to initiate the *movement execution* phase. In the saccade trials, participants shifted their gaze to fixate towards the remembered target location until hearing a second "beep", which prompted a return to central fixation. In the reach trials, participants touched the

board with their right index finger at the remembered target position while maintaining central fixation, holding that position until the return signal prompted them to move their right arm back to the button box. Finally, in the colour condition, participants maintained central fixation while indicating target colour by pressing the home button with their right index finger, once for green and twice for red. The response window of the movement execution phase was 2.4 seconds, after which a 12-second intertrial interval began. Each complete trial was 31.2 seconds.

Each functional run consisted of 12 trials (four per condition). Different trial types (saccade, reach, colour-report) were presented in a random order, with 50% of peripheral targets presented in each visual hemifield for each condition. No two trials repeated the same identical condition. Each session consisted of eight functional runs inside the scanner, with a break between the 4th and 5th run.

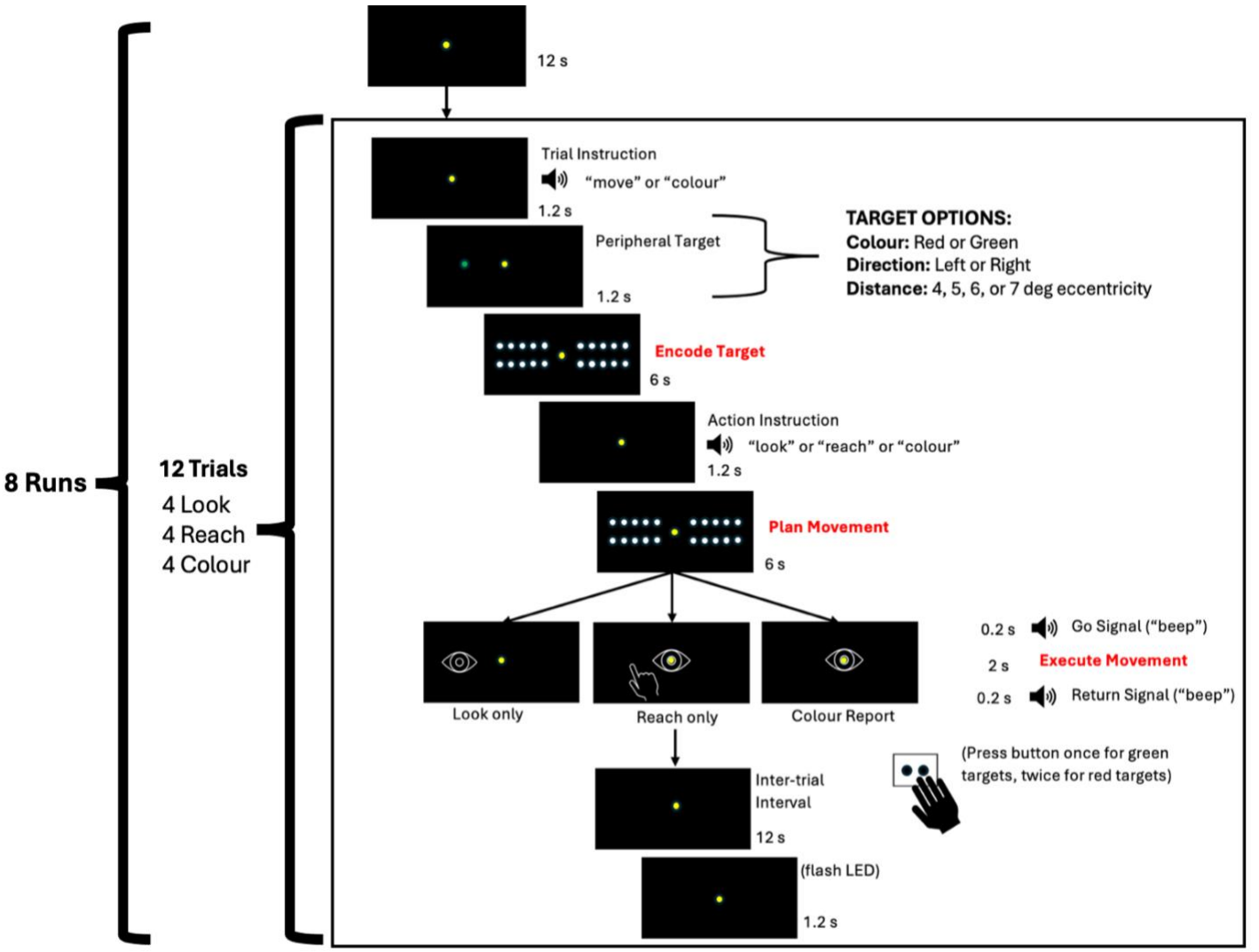


Figure 8: Illustration of the experimental paradigm. Visual stimuli on black screens represent participants' view within each timeframe of a single trial. The difference between the two experimental conditions (Saccade and Reach) emerged from the auditory instructions, which dictated the movements participants performed towards the remembered target position. The control condition (colour-report) required participants to remember the colour of the peripheral target and report it using the button box.

2.4 Training and Behavioural Recordings

Participants attended a training session at the MRI Simulator Facility at the Sherman Health Sciences Centre at York University at least 24 hours prior to the scan, which lasted approximately 30 minutes. During this time, we first confirmed with participants whether they were able to remain in the scanner for the entire duration of the experiment. We then explained the task and had them complete a few practice trials using the experimental

equipment until they were confident they understood the task. In addition to this, prior to scanning participants on the day of, they completed an additional run outside of the MRI bore, referred to as "Run 0." This allowed us to ensure that participants performed the task correctly and have a record of consistent behaviour in cases where eye-tracking was lost inside the scanner. Prior to Run 0, the position of the eye-tracker was adjusted to allow for viewing of the left-eye. Pupil and corneal reflection thresholds were adjusted on the EyeLink host computer, and a custom calibration task was employed to capture the x and y position of the pupil on the board. During calibration, participants sequentially fixated on 7 LEDs for 2 seconds each, with each position shown twice, achieving an average accuracy of 0.25-0.5 degrees (SR Research Ltd., 2025). The touchscreen recorded time and location of the reach end point. The behavioural information for one representative participant (Sub19) during Run 0 is shown in **Appendix A** and **Appendix B**.

2.5 Imaging Parameters

The scanning sessions took place at the York MRI Facility at the Sherman Health Sciences Centre at York University with a 3-T Siemens Magnetom TIM Trio scanner. The posterior section of a 12-channel head coil (6 channels) was positioned behind the participant's head and 4-channel flex coil over the front.

Functional images were collected using an echo-planar imaging (EPI) sequence (repetition time (TR) = 1200 ms; echo time (TE) = 30 ms; flip angle (FA) = 66°; field of view (FoV) = 240 mm x 240 mm; matrix size = 96 x 96, producing an in-plane resolution of 2.5 x 2.5 mm; slice thickness = 3 mm; no gap; 54 transverse slices captured in an interleaved order). Acquisition time was 9 minutes and 22 seconds.

Structural, T1-weighted (T1-w) images were acquired using an MPRAGE sequence (TR = 2300; TE = 2.26 ms; inversion time (TI) = 900 ms; FA = 8°; FoV = 256 x 256; matrix size = 256 x 256, producing an in-plane resolution of 1.0 mm x 1.0 mm; slice thickness = 1.0 mm; no gap; 192 sagittal slices captured in an ascending order) for whole brain structural imaging. Acquisition time was 5 minutes and 21 seconds.

To correct for distortion, dual-echo gradient field maps were acquired using a GRE sequence (TR = 566 ms; TE1 = 4.92 ms; TE2 = 7.38 ms; FA = 60°; FoV = 240 mm x 240 mm; matrix size = 96 x 96, producing an in-plane resolution of 2.5 x 2.5 mm; slice thickness = 3mm; no gap; 54 transverse slices captured in an interleaved order). Acquisition time was 1 minute and 51 seconds.

2.6 Preprocessing

Data preprocessing was conducted using fMRIPrep (Version 24.1.1; Esteban et al. 2018; 2019) and FMRIB Software Library (FSL; Version 6.00; Jenkinson et al., 2012). T1-w scans were skull-stripped using deepbet (Fisch et al., 2024) before participant-level pre-processing on all functional and anatomical data was executed using fMRIPrep. fMRIPrep performed minimal preprocessing, including non-uniformity correction, brain masking of the T1-w image, tissue segmentation, head-motion correction of the functional images, susceptibility distortion correction using acquired field-maps, co-registration of each functional run to the T1-w image using boundary-based registration, and nonlinear spatial normalization of T1-w (and consequently the functional scans) to standard MNI template space (MNI152Lin6Asym). Following fMRIPrep, each preprocessed BOLD run was skull-stripped prior to running additional preprocessing and processing in FSL's FEAT. Additional pre-processing in FSL during first-level analysis included spatial smoothing (8 mm Full Width at Half Maximum (FWHM)) and high-pass temporal filtering (100 s).

2.7 Data Analysis

2.7.1 Behavioural Analysis and Exclusion Criteria

To ensure participants correctly performed the instructed tasks during each trial, the event timing files for functional runs were examined offline. A trial was excluded from analysis if: 1) an uninstructed reach behaviour was recorded (e.g., participants touched the board for a colour-report trial) and 2) no action was recorded (e.g., participants did not reach to touch the board). In four participants, equipment issues prevented touch-end points from being recorded, despite participants reaching and touching the board with their index finger. In such cases, we verbally confirmed with participants that they had indeed touched the board

for reach trials following each run, although we were not able to verify behaviour further from this. Reach trials were not excluded for these scanning sessions. Additionally, the eye was monitored in real-time from the EyeLink Host monitor during the scan to confirm that participants were awake and performing the task. Although the eye-tracking camera was active during the scanning session, the setup did not provide optimal illumination and positioning for complete gaze tracking data during scans for any participant. Thus, we could not remove trials based on this data. Instead, eye-tracking data from Run 0 served as confirmation that participants were able to comply with the behavioural requirements of the task (i.e., fixate during trials and shift gaze during saccade execution).

Trials were also excluded if framewise displacement (FD) exceeded 0.99 mm inside the scanner outside the execution and inter-trial interval (ITI) phases. Runs were excluded if more than five trials, or more than two from the same condition, were removed due to head motion.

Due to technical malfunctions, four participants did not complete eight function runs inside the scanner, and data was not recorded for 10 runs in total (Sub01: three, Sub09: one, Sub12: four, sub21: two). Following preprocessing, one participant was excluded due to excessive head motion (all eight runs; 128 trials), leaving 19 participants (142 runs; 1704 trials) for final analysis. Of these, 32 trials (1.88%), including two entire runs, were removed due to excessive motion, with a mean of 1.68±4.32 trials per participant. Additionally, 43 trials (2.52%) were removed due to behavioural errors, with a mean of 2.26±1.66 trials per participant. Maximum number of trials excluded for a participant included in the analysis was five. In total, 75 trials (4.40%) were excluded across 19 participants, with a mean of 3.95±4.47 trials per participant, leaving 140 runs and 1629 trials for final analysis.

2.7.2 Univariate Analysis

Functional data was analyzed using FSL (Version 6.00; Woolrich et al., 2001). Peripheral target locations were pooled across left and right directions as laterality was not a factor of interest in the following analyses. Functional runs were fitted to three separate general linear models (GLMs) to examine task-related activation during 1) *visual target encoding* 2)

movement planning and 3) *movement execution* phases. For the *visual target encoding* phase, two predictors were defined based on condition: *Move* and *Colour*. One contrast was created to examine activation for encoding the spatial location of target for future movement versus encoding non-spatial properties for reporting colour: Contrast 1 [Move>Colour]. For the *movement planning* phase, three predictors were defined based on condition: *Reach*, *Saccade*, and *Colour*. Two contrasts were designed to investigate effector-related activation during saccade and reach planning compared to colour-report (control): Contrast 2 [Saccade>Colour] and Contrast 3 [Reach>Colour], and additional two contrasts were defined to investigate regions with greater activity for one effector over the other (effector-specificity contrasts): Contrast 4 [Saccade>Reach] and Contrast 5 [Reach>Saccade]. An identical GLM was set up for the *movement execution* phase (Contrasts 6 to 9). White matter time series (derived from fMRIPrep) was included as a nuisance regressor.

Parameter estimates were combined across runs within each participant using a fixed-effects model. Group-level statistical inference was performed using FSL randomise (Winkler et al., 2014), which performed voxel-wise non-parametric permutation testing (5000 permutations) with threshold-free cluster enhancement (TFCE; Smith et al., 2009) and family-wise error (FWE) correction ($p<0.05$). The *cluster* function on FSL was used to report cluster information for each contrast. Group level thresholded statistical maps were projected from volumetric MNI152 space onto FreeSurfer fsaverage surface using mri_vol2surf registration for visualization.

The anatomical location of cortical peak voxels and relevant local maxima were labelled using probabilistic atlases in volumetric space: the Harvard-Oxford Cortical Structural Atlas and Harvard-Oxford Subcortical Structural Atlas, provided by the Harvard Centre for Morphometric Analysis. The probability values reflect the proportion of individuals in the atlas sample for whom a given voxel was assigned to a particular region (FMRIB Software Library, n.d.). Cerebellar areas were identified using the Cerebellar Atlas in MNI152 space after normalization with FNIRT. All peak voxels were labelled unless they were too small (i.e., less than 10 voxels) or predominantly in white matter regions. Additionally, some local

maxima within clusters were labelled to provide further information on the extent of regions activated for each contrast. To estimate the location of MNI coordinates on the fsaverage inflated brain, a publicly available Yeo Lab function was used, which performs precomputed volumetric to surface mapping and outputs corresponding surface vertex values (Wu et al., 2018). Since the anatomical labels were derived from volume space, their spatial location appeared slightly shifted in some cases on the cortical surfaces.

2.7.3 Conjunction Analysis

To identify regions that are activated for both reach and saccade during the *movement planning* and *movement execution* phases, binary masks of the TFCE-corrected, t-statistic maps (thresholded at FWE $p<0.05$) for [Saccade>Colour] and [Reach>Colour] contrasts were generated. These binary maps were multiplied voxel-wise using *fslmaths*, to produce a conjunction map of overlapping areas.

2.7.4 Region of Interest Analysis

To further determine activity across key regions in the parieto-frontal cortex, regions of interest (ROIs) were selected using coordinates reported in previous literature. These included: bilateral anterior cingulate cortex (aCing); bilateral dorsolateral prefrontal cortex (DLPFC); supplementary eye field (MedFG); bilateral frontal eye field (MidFG); bilateral primary motor cortex (M1); bilateral dorsal premotor cortex (PMd); bilateral angular gyrus (AG); bilateral superior parieto-occipital cortex (SPOC); bilateral medial intraparietal sulcus (mIPS); bilateral primary somatosensory cortex (S1); bilateral primary visual cortex (V1). The MNI coordinates and corresponding references used for these regions is shown in **Table 1**.

Table 1: Name of regions selected for ROI analysis, hemisphere, MNI coordinates, and corresponding references.

Region	Hemisphere	MNI X	MNI Y	MNI Z	References
aCing	Left	-4	16	32	Jamadar et al., (2013)
aCing	Right	6	8	38	Jamadar et al., (2013)

DLPFC	Left	-38	34	36	Cameron et al., (2015)
DLPFC	Right	32	40	34	Jamadar et al., (2013)
MedFG		-2	-10	64	Jamadar et al., (2013)
MidFG	Left	-40	-14	54	Jamadar et al., (2013)
MidFG	Right	40	-8	54	Jamadar et al., (2013)
M1	Left	-39	-23	59	Sartin et al., (2023)
M1	Right	35	-25	64	Sartin et al., (2023)
PMd	Left	-25	-10	61	Cappadocia et al., (2017)
PMd	Right	22	-11	64	Cappadocia et al., (2017)
AG	Left	-40	-70	44	Vesia et al., (2010)
AG	Right	35	-75	46	Vesia et al., (2010)
SPOC	Left	-10	-85	46	Vesia et al., (2010)
SPOC	Right	9	-85	45	Vesia et al., (2010)
mIPS	Left	-22	-68	45	Vesia et al., (2010)
mIPS	Right	22	-66	45	Vesia et a., (2010)
S1	Left	-40	-28	52	Mayka et al., (2006) Blohm et al., (2019)
S1	Right	38	-30	42	Mayka et al., (2006) Blohm et al., (2019)
V1	Left	-6	-80	10	Desouza et al., (2003)
V1	Right	9	-79	8	Desouza et al., (2003)

Spherical ROIs (6 mm radius) were created at the centre of each coordinate using FSL to generate binary masks for each region. For each participant and contrast, ROIs were restricted to voxels within the subject-specific brain mask generated during higher-level FEAT analysis. ROI statistics were extracted for [Saccade>Colour] and [Reach>Colour] contrasts (Contrasts 2-3 and 6-7) using *featquery*, which computed percent signal change for contrast of parameter estimates (COPEs) within each masked ROI.

2.7.5 Statistical Analysis

Statistical tests were performed using R (Version 4.5.3). To determine whether activation significantly differed from the colour condition, mean percent signal change for each contrast within each region and phase was assessed using one-sample, two-sided t-tests.

P-values were corrected using false discovery rate (FDR) to control for multiple comparisons. To directly compare activation between effectors (saccades [Saccade>Colour] versus reaches [Reach>Colour]), percent signal change for each region was assessed using paired t-tests. P-values were corrected using FDR within each phase.

CHAPTER 3: RESULTS

3.1 Effector versus colour activation across encoding, planning, and execution

The first objective of this study was to characterize saccade and reach activation across the *visual target encoding*, *movement planning*, and *movement execution* phases. Contrast 1 ([Move>Colour]) was used for the *visual target encoding* phase and contrasts 2, 3, 6, and 7 ([Saccade>Colour] and [Reach>Colour]) were used for the effector-dependent phases. **Table 2** provides the list of abbreviations used in the labelling cortical regions, as well as references for previous saccade and reach- fMRI studies that have reported activation in these areas.

Table 2: List of brain region abbreviations and saccade or reach-related fMRI literature that have reported activation in these areas.

Region	Abbreviation	References
Occipital		
Lateral Occipital Cortex	LOC	Filimon et al. (2009)
Occipital Fusiform Gyrus	Occipital Fus.	Corbetta et al. (1998)
Lingual Gyrus	LG	Cappadocia et al. (2017)
Temporal		
Superior Temporal Gyrus	STG	Geier et al. (2006)
Temporal Pole	TP	N/A
Temporal Fusiform Cortex	Temporal Fus.	Corbetta et al. (1998)
Parietal		
Superior Parietal Lobule	SPL	Hertz and Fiehler (2015)
Angular Gyrus	AG	Astafiev et al. (2003)
Supramarginal Gyrus	SMG	Filimon et al. (2009)
Precuneus	PCu	Filimon et al. (2009)
Frontal		
Middle Frontal Gyrus	MidFG	Grier et al. (2007)
Superior Frontal Gyrus	SFG	Filimon et al. (2009)
Frontal Pole	FP	Hertz and Fiehler (2015)

Cingulate		
Anterior Cingulate Cortex	aCing	Astafiev et al. (2003)

3.1.1 Visual Target Encoding

During the *visual target encoding* phase, participants were instructed on whether they needed to remember the position of the target to perform a movement towards it, or its colour to report. Since there were no instructions on if the movement would require the hand or the eyes, clusters surviving the [Move>Colour] contrast could be related to spatial-working memory or effector-independent movement preparation. **Figure 9** shows the functional map of significant regions, overlaid on the fsaverage inflated cortical surface. **Table 3** reports the MNI coordinates and t-statistic values of peak voxels from significant clusters. During this phase, activation was limited to the left hemisphere, with peak voxels in the TP, STG, and anterior and posterior MidFG.

In summary, greater activation during the *visual target encoding* phase for memory-guided movements was modest and limited to left temporal and middle frontal regions relative to the non-spatial task.

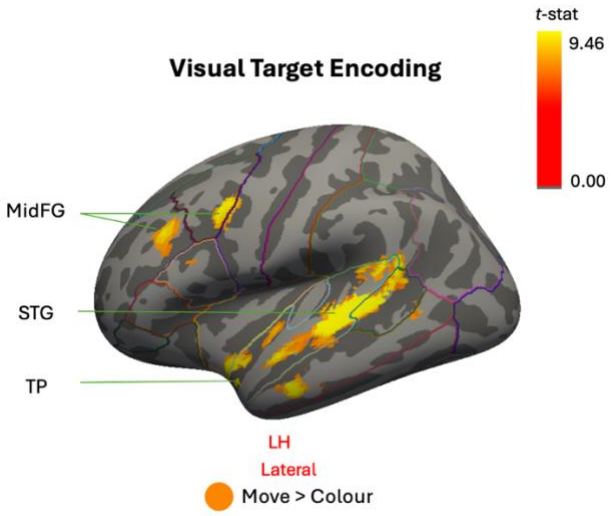


Figure 9: Group-level activation for the visual target encoding phase ([Move>Colour] contrast) overlaid on the FreeSurfer fsaverage 'inflated' cortical surface. Light gray represents gyri and dark gray represents sulci. Lines on the surface denote the anatomical

boundaries from the Desikan-Killiany Atlas, provided for visualization. Highlighted regions represent significant voxels from TFCE-corrected t-statistic maps (FWE $p<0.05$), with the colour-gradient corresponding to the magnitude of the t-statistic, as indicated by the colour bar. Labels are peak voxels.

Table 3: Name of region, hemisphere, MNI coordinates, t-statistic at the coordinate, and cluster sizes (number of voxels) for the visual target encoding phase ([Move>Colour] contrast).

Cluster	Region	Hemisphere	MNI X	MNI Y	MNI Z	t-stat	Voxels
1	STG	Left	-64	-20	0	9.46	1606
2	MidFG	Left	-38	6	34	5.72	282
3	MidFG	Left	-48	30	30	5.32	217
4	TP	Left	-42	8	-18	8.27	78

3.1.2 Movement Planning

During the *movement planning* phase, participants were aware of the required effector (eye vs. hand). Thus, the contrasts [Saccade>Colour] and [Reach>Colour] isolate effector-dependent planning activity relative to preparing for a button-press (colour-report condition). **Figure 10** shows these cortical functional maps, overlaid on the fsaverage inflated cortical surface. **Table 4** reports the MNI coordinates and t-statistic values of peak voxels, along with select local maxima within each significant cluster to illustrate the spatial extend of activation. Saccade planning produced activation primarily across posterior parietal regions (**Figure 10A**). The largest cluster (1041 voxels) revealed peak and local maximum activity in the left anterior and posterior SPL. A smaller homologous cluster (262 voxels) was observed in the right hemisphere, with peak activity in right SPL and local maximum within PCu. Additionally, a smaller cluster (22 voxels) was present in the left precentral gyrus. Conversely, reach planning was characterized by a single, large cluster (80445 voxels), spanning the occipital-parietal-frontal cortex (**Figure 10B**). The peak voxel was located in the left SPL, and local maxima were present in frontal regions, specifically the SFG and FP.

Overall, while both effectors revealed cortical engagement during this effector-dependent phase, activation differed. Saccade planning activity was relatively more focal along posterior parietal areas whereas reach planning was characterized by substantially broader and stronger activation along the cortex, with peaks in left posterior parietal and frontal regions.

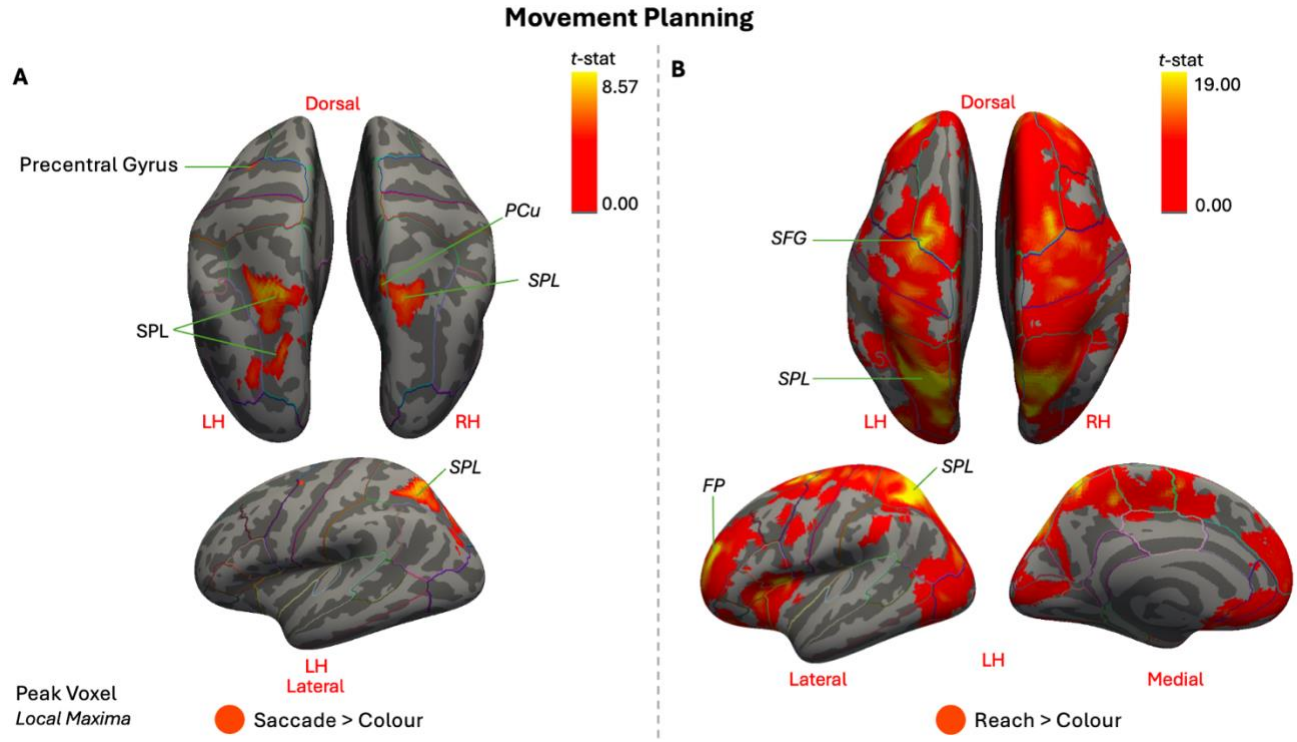


Figure 10: Group-level activation during the movement planning phase for the [Saccade>Colour contrast (panel A) and [Reach>Colour] contrast (panel B). Cortical results are overlaid on the FreeSurfer fsaverage 'inflated' brain. Light gray represents gyri and dark gray represents sulci. Lines on the surface denote the anatomical boundaries from the Desikan-Killiany Atlas, provided for visualization. Highlighted regions represent significant voxels from TFCE-corrected t-statistic maps (FWE $p<0.05$), with the colour-gradient corresponding to the magnitude of the t-statistic, as indicated by the colour bar. Labels are peak voxels and local maxima within clusters (local maxima shown in smaller italics).

Table 4: Name of region, hemisphere, MNI coordinates, t-statistic at the coordinate, and cluster sizes (number of voxels) for the movement planning phase ([Saccade>Colour] and [Reach>Colour] contrasts).

Cluster	Region	Hemisphere	MNI X	MNI Y	MNI Z	*t*-stat	Voxels
Saccade>Colour							
1	SPL	Left	-18	-62	56	8.57	1041

	SPL	Left	-24	-58	54	8.08	
2	SPL	Right	16	-66	56	6.72	262
	PCu	Right	8	-60	58	6.65	
3	Precentral Gyrus	Left	-36	-10	44	6.03	22
Reach>Colour							
1	SPL	Left	-22	-60	58	19	80445
	FP	Left	-26	42	16	14.4	
	SFG	Left	-22	-6	60	11.6	

3.1.3 Movement Execution

During the *movement execution* phase, participants performed the instructed movement (saccade or reach) towards the remembered target position. Consequently, the contrasts [Saccade>Colour] and [Reach>Colour] isolate regions with greater activity during effector-dependent movement, relative to the colour-report condition. **Figure 11** displays the cortical functional maps of these contrasts, overlaid on the fsaverage inflated cortical surface and **Table 5** reports the MNI coordinates and t-statistic values of peak voxels and local maxima with each significant cluster. Saccade execution (**Figure 11A**) revealed distributed occipital, posterior parietal, and frontal activation. The largest cluster's (43982 voxels) peak activity was centered in the Occipital Fus. and extended into bilateral SPL and left PCu. Additionally, a second large cluster (10753 voxels) was centered in the left precentral gyrus, with a local maximum in right precentral gyrus. Finally, a smaller cluster revealed peak activity in the FP. In contrast, reach execution was dominated by a large cluster (69814 voxels) with activation that extended into occipital, parietal, and frontal regions, including local peak activity in the left postcentral gyrus (**Figure 11B**). Activation in this cluster was stronger in the left hemisphere. An additional smaller cluster (195 voxels) was observed more laterally, centered in the left precentral gyrus.

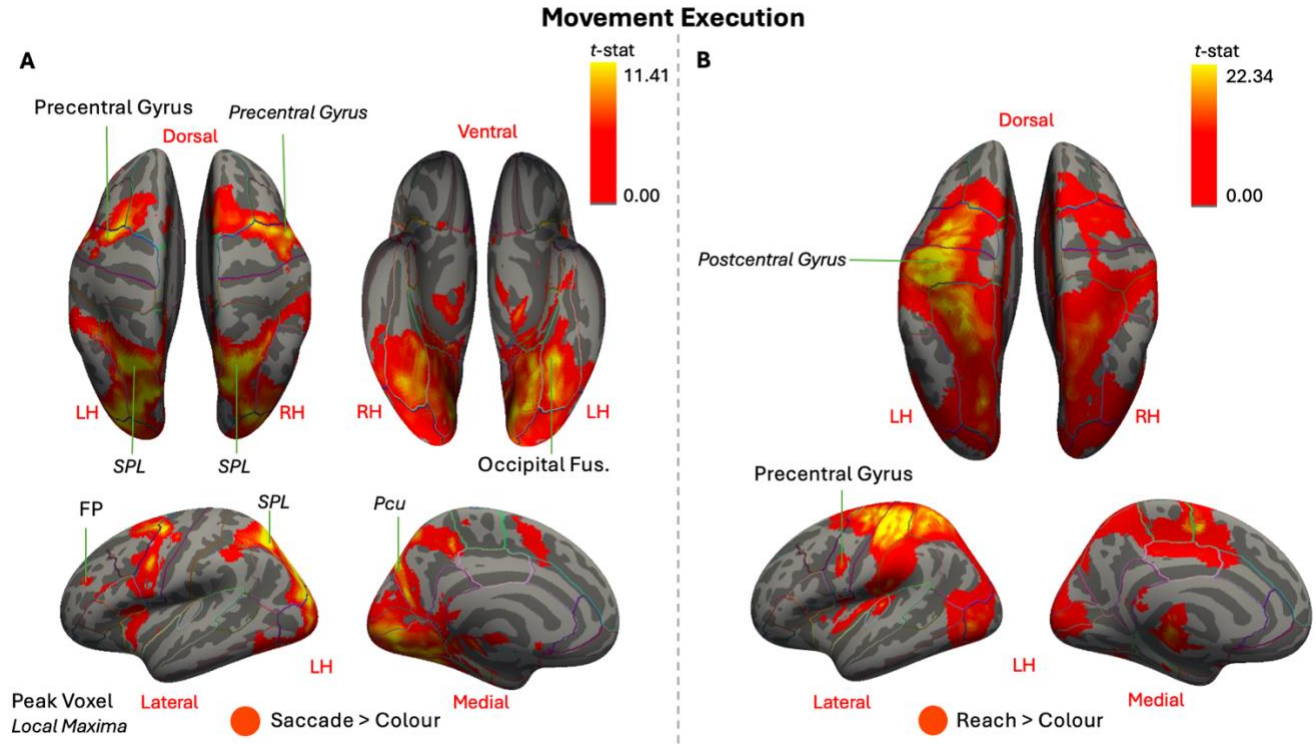


Figure 11: Group-level activation during the movement execution phase for the [Saccade>Colour] contrast (panel A) and [Reach>Colour] contrast (panel B). Cortical results are overlaid on the FreeSurfer fsaverage 'inflated' cortical surface. Light gray represents gyri and dark gray represents sulci. Lines on the surface denote the anatomical boundaries from the Desikan-Killiany Atlas, provided for visualization. Highlighted regions represent significant voxels from TFCE-corrected t-statistic maps (FWE $p<0.05$), with the colour-gradient corresponding to the magnitude of the t-statistic, as indicated by the colour bar. Labels are peak voxels and local maxima within clusters (local maxima shown in smaller italics).

Importantly, *movement execution* phase contrasts [Saccade>Colour] and [Reach>Colour] revealed cerebellar activity, shown in **Figure 12**. During saccade execution (**Figure 12A**) there was modest cerebellar activation although no peaks were observed. In contrast, the largest cluster during reach execution (69814 voxels) had its peak activity in the right lobule V and VIIIb, as well as a local maxima extending into the vermis VIIIa (**Figure 12B**).

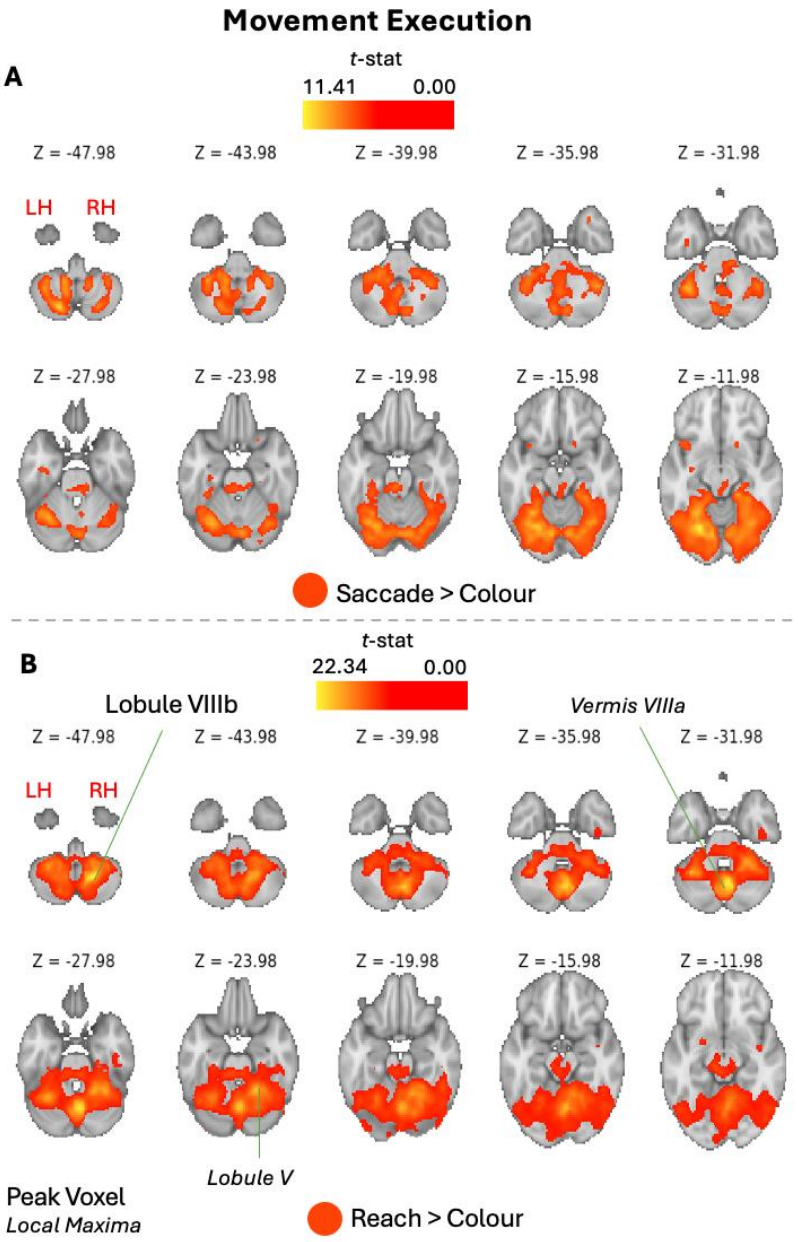


Figure 12: Group-level activation during the movement execution phase for the [Saccade>Colour] contrast (panel A) and [Reach>Colour] contrast (panel B). Cerebellar results are displayed on the MNI152 standard brain, shown as horizontal slices at every fourth axial z-slice in volume space. Highlighted regions represent significant voxels from TFCE-corrected t-statistic maps (FWE $p<0.05$), with the colour-gradient corresponding to the magnitude of the t-statistic, as indicated by the colour bar. Labels are peak voxels and local maxima within clusters (local maxima shown in smaller italics).

Altogether, both effectors produced widespread cortical activity with clear differences during the *movement execution* phase. Saccade execution was characterized with peaks in

occipital, posterior parietal, and frontal areas. Although cerebellar activity was present, no peak voxels were observed. Similar to the *movement planning* phase, reach execution produced broader and stronger activity that was predominantly left-lateralized, especially along the postcentral gyrus and adjacent precentral gyrus, consistent with limb-movement related areas (Beurze et al., 2007). Reach execution also revealed peaks of the right cerebellum and the vermis.

Table 5: Name of region, hemisphere, MNI coordinates, t-statistic at the coordinate, and cluster sizes (number of voxels) for the movement execution phase ([Saccade>Colour] and [Reach>Colour] contrasts).

Cluster	Region	Hemisphere	MNI X	MNI Y	MNI Z	*t*-stat	Voxels
Saccade>Colour							
1	Occipital Fus.	Left	-24	-68	-12	11.4	43982
	SPL	Left	-26	-60	48	10.6	
	SPL	Right	28	-58	52	10.4	
	Pcu	Left	-18	-76	40	10.6	
2	Precentral Gyrus	Left	-32	-8	46	10.2	10753
	Precentral Gyrus	Right	52	2	42	9.78	
3	FP	Left	-42	44	30	4.42	61
Reach>Colour							
1	Lobule VIIIb	Right	18	-58	-48	22.3	69814
	Vermis VIIIa		6	-64	-30	22.2	
	Postcentral Gyrus	Left	-40	-26	62	18	
	Lobule V	Right	20	-46	-24	16.9	
2	Precentral Gyrus	Left	-54	2	32	9.3	195

3.2 Overlapping saccade and reach activation during planning and execution

Our next goal was to better understand the commonalities between saccade and reach activation during the planning and execution phases.

3.2.1 Movement Planning

The *movement planning* phase for the [Saccade>Colour] contrast revealed peak activity along bilateral posterior parietal regions and in the left precentral regions, whereas the [Reach>Colour] contrast showed more widespread activity, with peaks posterior parietal and frontal regions (**Figure 11**). The overlap of these two maps ([Saccade>Colour] ∩ [Reach>Colour]) is presented in **Figure 13**, overlaid on the fsaverage inflated cortical surface. The most immediate observation is the strong similarity between the overlapping and [Saccade>Colour] contrast maps. Notably, all significant peak voxels and local maxima identified during saccade planning were present in this conjunction map. Thus, overlapping activation during reach and saccade planning is observed bilaterally in SPL, as well as in the right PCu and left precentral gyrus. Importantly, the results here simply identify voxels that were significant in both contrasts, but it does not provide information about the relative strength of activation.

In summary, overlapping activation for the saccade and reach condition was mostly revealed along bilateral posterior parietal areas during the *movement planning* phase. The spatial pattern of overlap closely matched what was observed during saccade planning while the broader cortical activity present during reach planning was not retained.

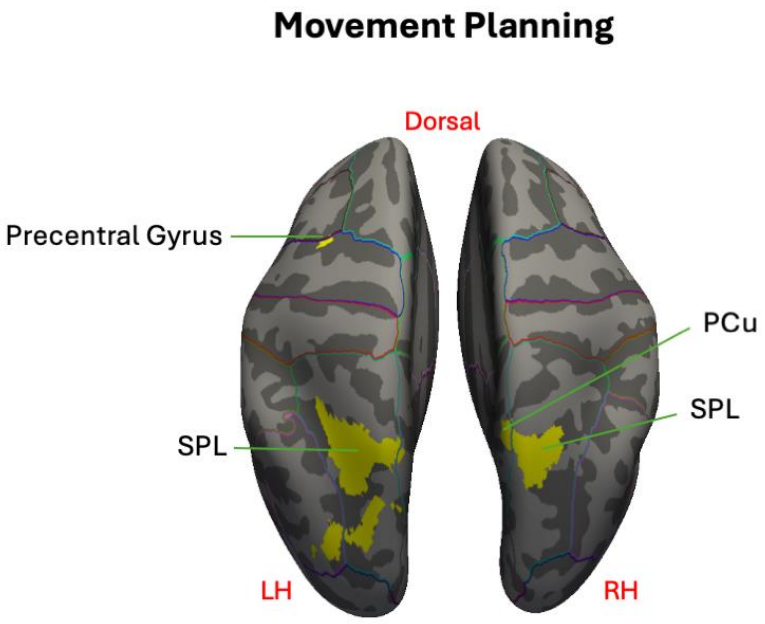


Figure 13: Overlapping activation for reach and saccade during the movement planning phase ([Saccade>Colour] ∩ [Reach>Colour]). Cortical results are overlaid on the FreeSurfer fsaverage 'inflated' cortical surface. Light gray represents gyri and dark gray represents sulci. Lines on the surface denote the anatomical boundaries from the Desikan-Killiany Atlas, provided for visualization. Highlighted regions represent voxels significant in both contrasts, suggesting possible involvement for both effectors. Coordinates for labels come from peak voxels and local maxima of [Saccade>Colour] contrast during the movement planning phase.

3.2.2 Movement Execution

During movement execution, the [Saccade>Colour] contrast revealed activity along occipital, posterior parietal, and frontal regions (**Figure 11A**). The [Reach>Colour] contrast revealed widespread activation along cerebellar and cortical areas, with peak activity localized within the posterior cerebellum, left postcentral gyrus and precentral gyrus (**Figure 11B; Figure 12B**). The cortical overlap of these two maps ([Saccade>Colour] ∩ [Reach>Colour]) is presented in **Figure 14**, overlaid on the fsaverage inflated cortical surface. Similar to the *movement planning* phase, overlapping cortical activation was similar to the functional map produced for saccade execution, with all significant peak voxels and local maxima identified during saccade execution present in this conjunction map. Thus, saccade and reach execution both engage the bilateral SPL, precentral gyrus, as well the left PCu.

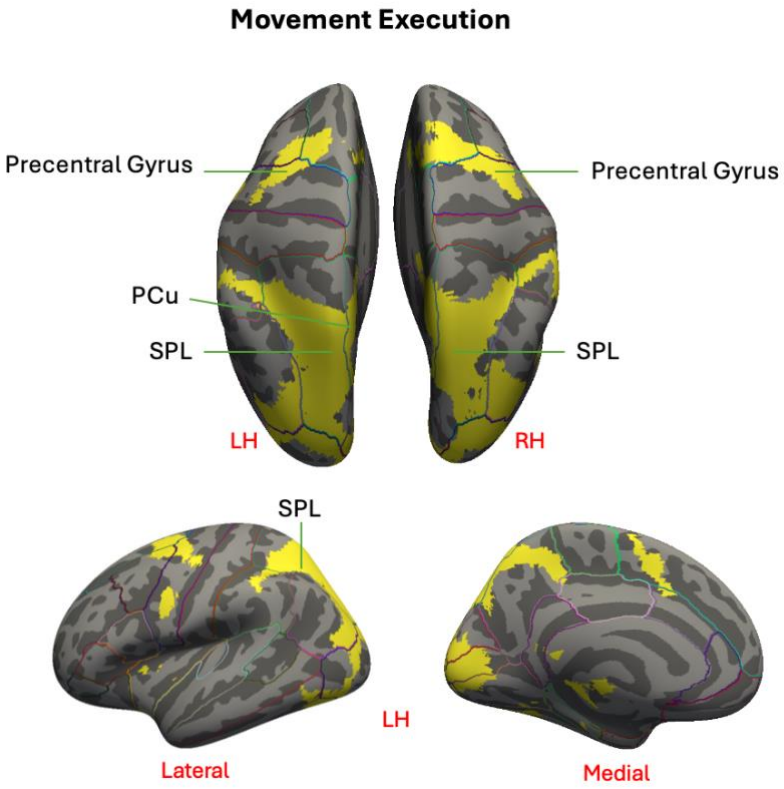


Figure 14: Overlapping activation for reach and saccade during the movement execution phase ([Saccade>Colour] ∩ [Reach>Colour]). Cortical results are overlaid on the FreeSurfer fsaverage 'inflated' cortical surface. Light gray represents gyri and dark gray represents sulci. Lines on the surface denote the anatomical boundaries from the Desikan-Killiany Atlas, provided for visualization. Highlighted regions represent voxels significant in both contrasts, suggesting possible involvement for both effectors. Coordinates for labels come from peak voxels and local maxima of [Saccade>Colour] contrast during the movement execution phase.

There was also overlap within cerebellar regions, shown in **Figure 15**, although engagement did not coincide with any of the peak and local maxima coordinates present within the [Reach>Colour] contrast, despite some overlap within the same anatomical regions. As a reminder, although activation did expand to cerebellar regions in the [Saccade>Colour] functional map, no peak voxels or local maxima were identified. Visual inspection of the conjunction map revealed overlapping activity within bilateral cerebellar lobules, including but not limited to lobule VI, Crus I, and lobule VIIIa, extending medially into the vermal VI and VIIIa (labelled in **Figure 15** for visualization). Once again, this analysis only provides

information about areas that were significantly active in both contrasts but does not account for the strength of activation during saccade and reach execution.

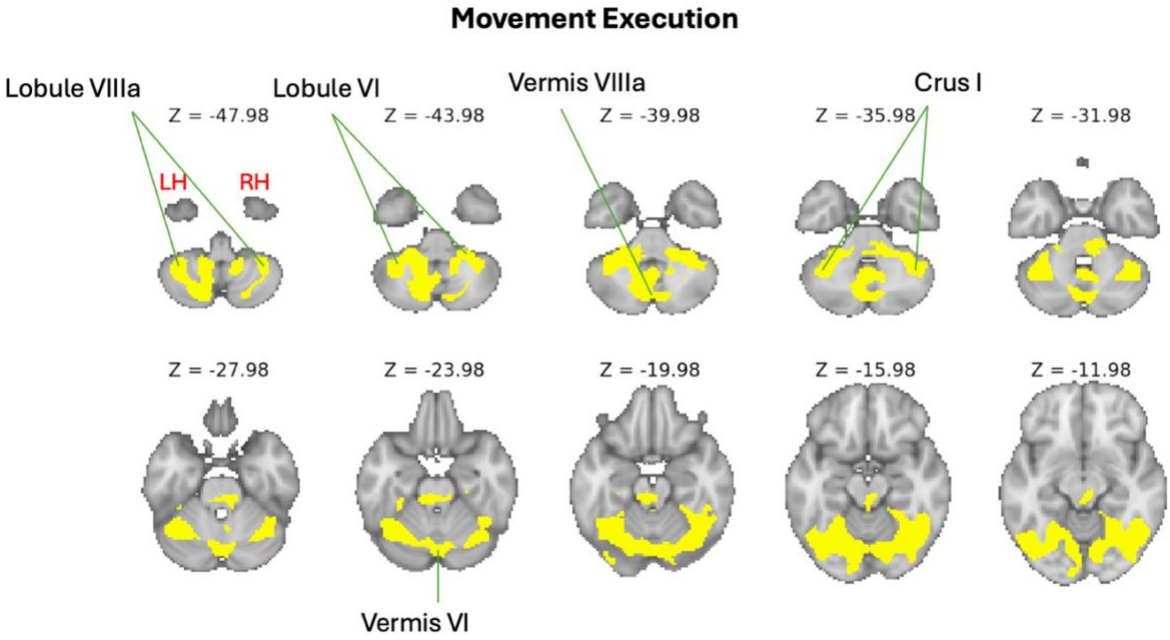


Figure 15: Overlapping activation for reach and saccade during the movement execution phase ([Look>Colour] ∩ [Reach>Colour]). Cerebellar results are displayed on the MNII152 standard brain, shown as horizontal slices at every fourth axial z-slice in volume space. Highlighted regions represent significant voxels from TFCE-corrected t-statistic maps (FWE $p<0.05$), with the colour-gradient corresponding to the magnitude of the t-statistic, as indicated by the colour bar. Labels are provided for visualization but do not correspond to peak voxels or local maxima of [Saccade>Colour] or [Reach>Colour] contrasts.

Overall, the *movement execution* phase showed overlapping activity between saccade and reach conditions in bilateral occipital, posterior parietal, and frontal areas, as well as broad cerebellar regions. Similar to *movement planning*, the overlap map closely resembled what was observed for saccade execution, although the more extensive activation observed during reach execution was not retained.

3.3 Effector-preferential activation across planning and execution

To determine regions with preferential activation for reach versus saccade movements, whole-brain contrasts that directly compared effectors were performed for the effector-dependent planning (contrasts 4 and 5) and execution phases (contrasts 8 and 9).

3.3.1 Movement planning

Direct [Saccade>Reach] and [Reach>Saccade] contrasts during the *movement planning* phase identified regions that are more strongly engaged for saccades versus reaches and vice versa, respectively. Functional maps of these contrasts, overlaid on the fsaverage inflated cortical surface, are presented in **Figure 16**. **Table 6** reports the MNI coordinates and t-statistic values of peak voxels and local maxima with each significant cluster. Saccade-preferential activation was characterized by a large cluster (15021 voxels) centered in the ventral occipitotemporal cortex. The peak voxel was centered in the left Temporal Fus. (**Figure 16A**), with activation extending into the right Temporal Fus. An additional, smaller cluster (208 voxels) was centered in the right LOC. In contrast, reach-preferential activation was dominated by a single, very large cluster (83599 voxels) that spanned bilateral occipital, parietal, and frontal regions. Peak activity for this cluster was present within the left SPL and extended to a local maximum in the left LOC (**Figure 16B**).

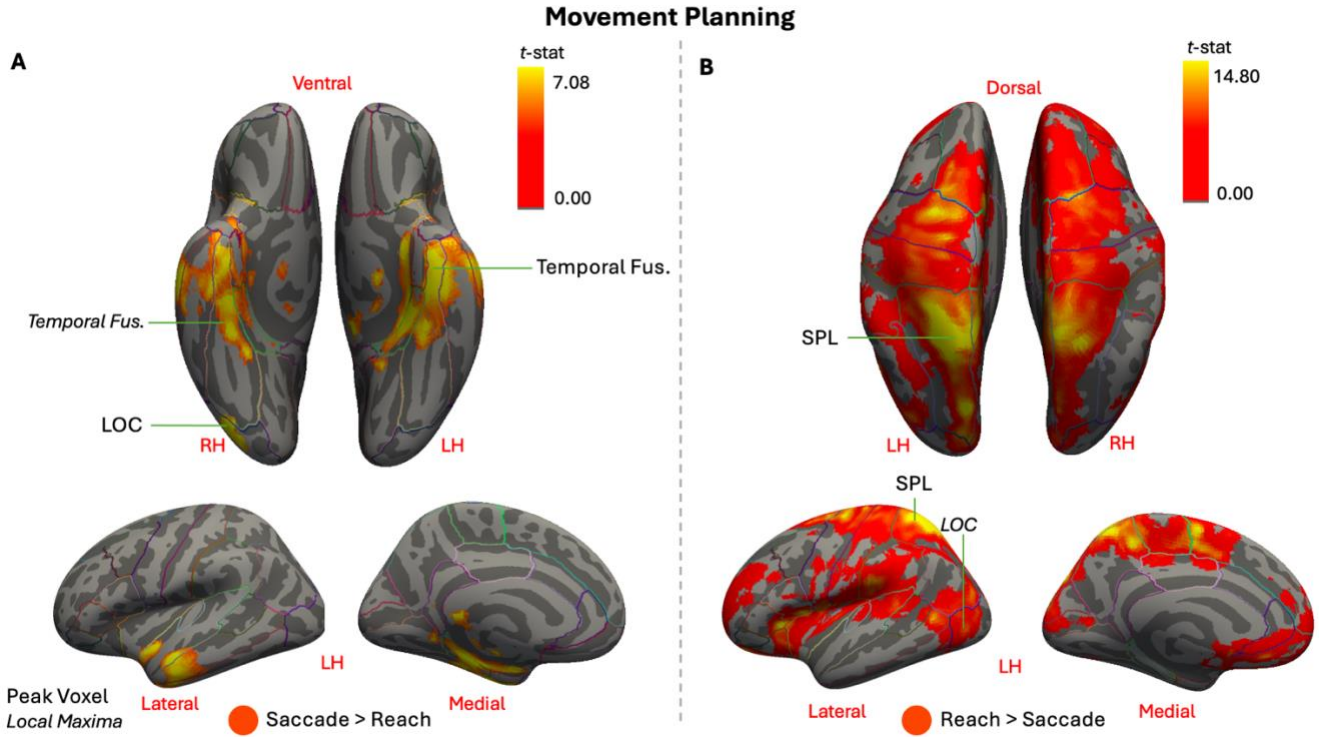


Figure 16: Group-level activation during the movement planning phase for the [Saccade>Reach] contrast (panel A) and [Reach>Saccade] contrast (panel B). Cortical results are overlaid on the FreeSurfer fsaverage 'inflated' cortical surface. Light gray represents gyri and dark gray represents sulci. Lines on the surface denote the anatomical boundaries from the Desikan-Killiany Atlas, provided for visualization. Highlighted regions

represent significant voxels from TFCE-corrected t-statistic maps (FWE $p<0.05$), with the colour-gradient corresponding to the magnitude of the t-statistic, as indicated by the colour bar. Labels are peak voxels and local maxima within clusters (local maxima shown in smaller italics).

Cerebellar activation for saccade-preferential and reach-preferential areas is shown in **Figure 17**. Saccade-related activity from cluster 1 extended into the left lobule I-IV (**Figure 17A**) while no reach-preferential cerebellum activity was observed during this phase (**Figure 17B**).

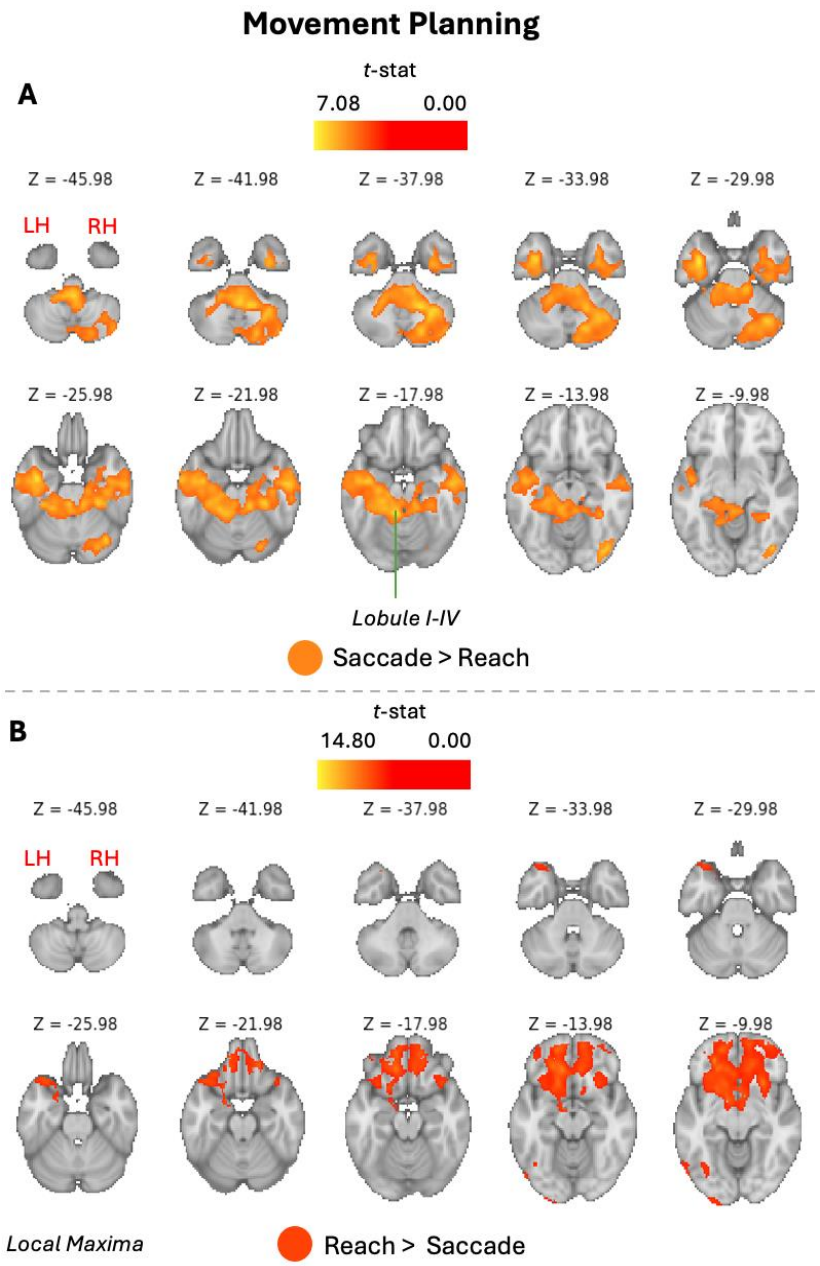


Figure 17: Group-level activation during the movement planning phase for the [Saccade>Reach] contrast (panel A) and [Reach>Saccade] contrast (panel B). Subcortical results are displayed on the MNII152 standard brain, shown as horizontal slices at every fourth axial z-slice in volume space. Highlighted regions represent significant voxels from TFCE-corrected t-statistic maps (FWE $p<0.05$), with the colour-gradient corresponding to the magnitude of the t-statistic, as indicated by the colour bar. Labels are peak voxels and local maxima within clusters (local maxima shown in smaller italics).

Overall, saccade- and reach- preferential activity was revealed during the planning phase, with distinct spatial organizations. Saccade-preferential activity was evident in the ventral

occipitotemporal cortex as well as the left cerebellum while reach-preferential activity produced broader and stronger cortical activity spanning dorsal occipital and posterior parietal regions. The findings here are consistent with the comparatively limited cortical recruitment observed during saccade planning relative to reach planning (**Figure 4**).

Table 6: Name of region, hemisphere, MNI coordinates, t-statistic at the coordinate, and cluster sizes (number of voxels) for the movement planning phase ([Saccade>Reach] and [Reach>Saccade] contrasts).

Cluster	Region	Hemisphere	MNI X	MNI Y	MNI Z	*t*-stat	Voxels
Saccade>Reach							
1	Temporal Fus.	Left	-38	-6	-28	7.08	15021
	Temporal Fus.	Right	30	-32	-24	6.18	
	Lobule I-IV	Left	-6	-42	-18	6.16	
2	LOC	Right	42	-76	-12	6.32	208
Reach>Saccade							
1	SPL	Left	-22	-60	60	14.8	83599
	LOC	Left	-16	-84	40	10.1	

3.3.2 Movement Execution

Similar to the *movement planning* phase, direct contrasts during movement execution identified regions with greater activity for saccades versus reaches, and vice versa. Functional maps for the [Saccade>Reach] and [Reach>Saccade] contrasts, overlaid on the fsaverage inflated cortical surface, are presented in **Figure 18**. **Table 7** reports the MNI coordinates and t-statistic values of peak voxels and local maxima with each significant cluster. Saccade-preferential activation was dominated by a large cluster (78018 voxels) with an activation pattern that spanned occipital, lateral parietal, and superior and middle frontal regions (**Figure 18A**). The peak voxel was located in the left Occipital Fus, with activation extending into left AG/SMG, left LOC, and left LG. Conversely, reach-preferential activation was present in a large cluster (38205 voxels) exhibiting a spatial pattern that spanned occipital, medial parietal, and frontal regions (**Figure 18B**). Local peak activity was

found in the left postcentral gyrus. A smaller cluster (543 voxels) was also present, centered in the left LOC.

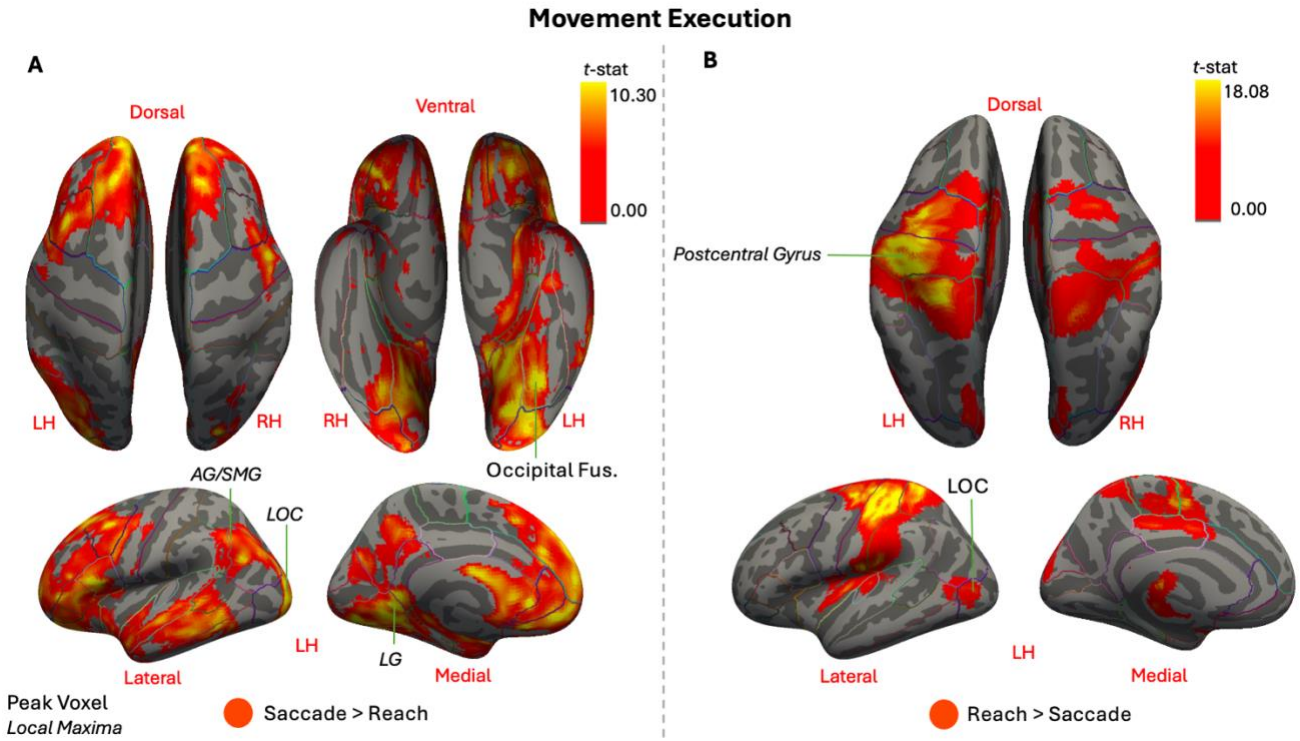


Figure 18: Group-level activation during the movement execution phase for the [Saccade>Reach] contrast (panel A) and [Reach>Saccade]) contrasts (panel B). Cortical results are overlaid on the FreeSurfer fsaverage 'inflated' cortical surface. Light gray represents gyri and dark gray represents sulci. Lines on the surface denote the anatomical boundaries from the Desikan-Killiany Atlas, provided for visualization. Highlighted regions represent significant voxels from TFCE-corrected t-statistic maps (FWE $p<0.05$), with the colour-gradient corresponding to the magnitude of the t-statistic, as indicated by the colour bar. Labels are peak voxels and local maxima within clusters (local maxima shown in smaller italics).

Figure 19 shows the cerebellar activation. Saccade-preferential activation in cluster 1 expanded into the cerebellum, although peak activity was not found here (**Figure 19A**). A smaller, focal cluster (18 voxels) was also present in the left lobule VIIb (not labelled). Conversely, reach-preferential activation in the largest revealed peak activity in the right lobule VIIIb, with a local maximum in the right lobule V (**Figure 19B**).

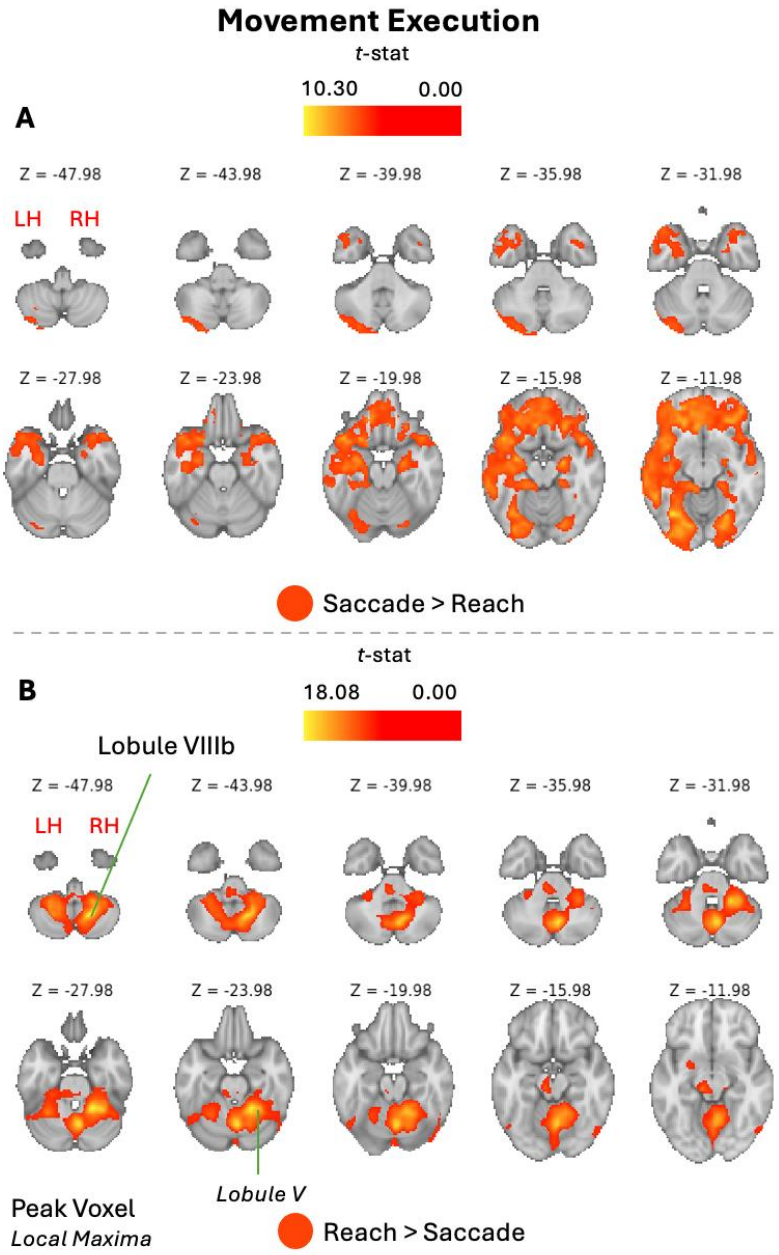


Figure 19: Group-level activation during the movement execution phase for the [Saccade>Reach] contrast (panel A) and [Reach>Saccade]) contrast (panel B). Subcortical results are displayed on the MNI152 standard brain, shown as horizontal slices at every fourth axial z-slice in volume space. Highlighted regions represent significant voxels from TFCE-corrected t-statistic maps (FWE $p<0.05$), with the colour-gradient corresponding to the magnitude of the t-statistic, as indicated by the colour bar. Labels are peak voxels and local maxima within clusters (local maxima shown in smaller italics).

In summary, effector-preferential differences were most pronounced during the *movement execution* phase. Saccade-preferential activity was concentrated mostly along ventral occipital and lateral posterior parietal regions, while reach-preferential activity showed a more medial and dorsal distribution spanning parietal and frontal spatial cortices, with peak activity in the left postcentral gyrus and right cerebellum. These patterns align with those observed during saccade and reach execution, respectively (**Figures 11-12**), where reach execution similarly revealed peak activity in the left postcentral gyrus and right cerebellum while saccade execution did not. However, through directly contrasting reach and saccade conditions, more medial-lateral spatial patterns emerged for activation along the PPC.

Table 7: Name of region, hemisphere, MNI coordinates, t-statistic at the coordinate, and cluster sizes (number of voxels) for the movement execution phase ([Saccade>Reach] and [Reach>Saccade] contrasts).

Cluster	Region	Hemisphere	MNI X	MNI Y	MNI Z	*t*-stat	Voxels
Saccade>Reach							
1	Occipital Fus.	Left	-34	-66	30	10.3	78018
	AG/SMG	Left	-60	-54	42	10.3	
	LOC	Left	-48	-76	36	10.3	
	LG	Left	-18	-52	0	9.98	
2	Lobule VIIb	Left	-30	-66	-50	3.55	18
Reach>Saccade							
1	Lobule VIIIb	Right	22	-56	-46	18.1	38205
	Lobule V	Right	20	-46	-26	18	
	Postcentral Gyrus	Left	-48	-20	52	18	
2	LOC	Left	-46	-74	4	8.67	543

3.4 Region-of-interest analysis

The comparison of saccade and reach activity with the colour-report condition revealed several occipital, parietal, and frontal regions exhibiting effector-dependent activity during planning and execution phases. Additionally, direct contrasts between these effectors identified cortical regions showing greater activation for reach versus saccade, and vice versa. However, to what extent do cortical regions show differences in activation between saccade and reach? To quantify these differences, a ROI analysis was conducted by comparing BOLD percent signal change for the [Saccade>Colour] and [Reach>Colour] contrasts within functionally defined regions (**Table 1**) consistently implicated in the literature for reach and saccade processing.

3.4.1 Movement Planning

Data shown in **Figure 20** illustrate the ROI analysis for the *movement planning* phase. Significant difference (paired *t*-test; FDR-corrected $p<0.05$) between saccade- and reach-related activity was observed in the right aCing, bilateral DLPFC, MedFG, bilateral MidFG, bilateral PMd, bilateral M1, left AG, left mIPS, and bilateral SPOC (**Figure 20A**). Of these, activity was significantly greater for saccades than the colour condition only in left mIPS, and significantly lower in left M1, left MidFG, MedFG, and left S1 (one-sample *t*-test, FDR-corrected $p<0.05$; **Figure 20B**). Reach activity was significantly greater than colour in all regions shown in **Figure 20B**, except left AG, right SPOC, left MidFG, and left S1. Critically, all of these areas showed significantly greater activation values for reach than saccade, indicating reach-preferential activity within these areas during movement preparation. This preference comes from the higher relative mean BOLD signal change for reaches compared with saccades, despite some regions showing larger effect magnitudes for saccades. The plots for all regions, including those with no significant saccade versus reach differences, are available in **Appendix C**.

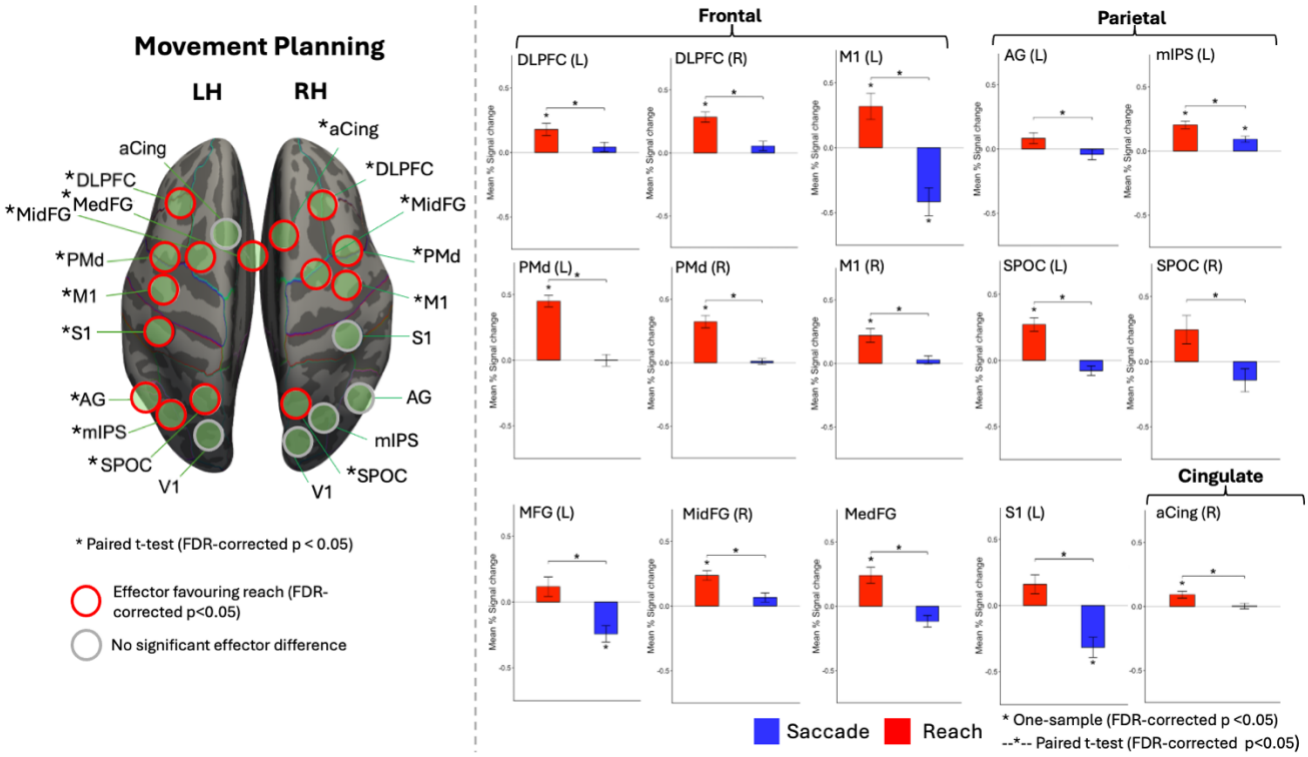


Figure 20: ROI analysis for selected regions during the movement planning phase. ROIs are displayed on the FreeSurfer fsaverage 'inflated' cortical surface (panel A). Asterisks beside ROI labels indicate a significant difference between the [Saccade>Colour] and [Reach>Colour] contrasts (paired *t*-test; FDR-corrected p<0.05). Red outlines identify ROIs with significantly greater mean % signal change values for reach compared to saccade, whereas gray outlines represent no significant difference between effectors. Mean % signal change for ROIs showing a significant effector difference is plotted (panel B). Asterisks above bars indicate significant one-sample effects (FDR-corrected p<0.05), and brackets denote significant differences between effectors from paired t-tests (FDR-corrected p<0.05). Red bars correspond to reach values and blue bars to saccade. Error bars represent SEM.

3.4.2 Movement Execution

Figure 21 reveals the ROI analysis for the *movement execution* phase. Significant difference (paired *t*-test; FDR-corrected p<0.05) between saccade- and reach-related activity was observed in the right aCing, left DLPFC, MedFG, left MidFG, bilateral PMd, left M1, left AG, left mIPS, bilateral SPOC, and right V1 (**Figure 21A**). Of these, activity was significantly greater for saccades than the colour condition in left mIPS, right V1, left SPOC and left PMd, and lower in left MidFG, left M1, and left S1 (one-sample *t*-test, FDR-corrected p<0.05; **Figure 21B**). Reach activity was significantly greater than the colour condition in all areas shown in **Figure 21B** except left AG, where activity was significantly lower. In contrast to the

movement planning phase, several regions showed significant differences favoring saccades, including right DLPFC, left AG, left mIPS, and left V1. However, note that in right DLPFC neither effector showed significant activity greater than the colour condition and in left AG both saccade- and reach-related activity were significantly lower than the colour condition, with saccades being significantly less negative than reach. All other significant regions favored reach-related activity. The plots for all regions, including those with no significant saccade versus reach differences, are available in **Appendix D**.

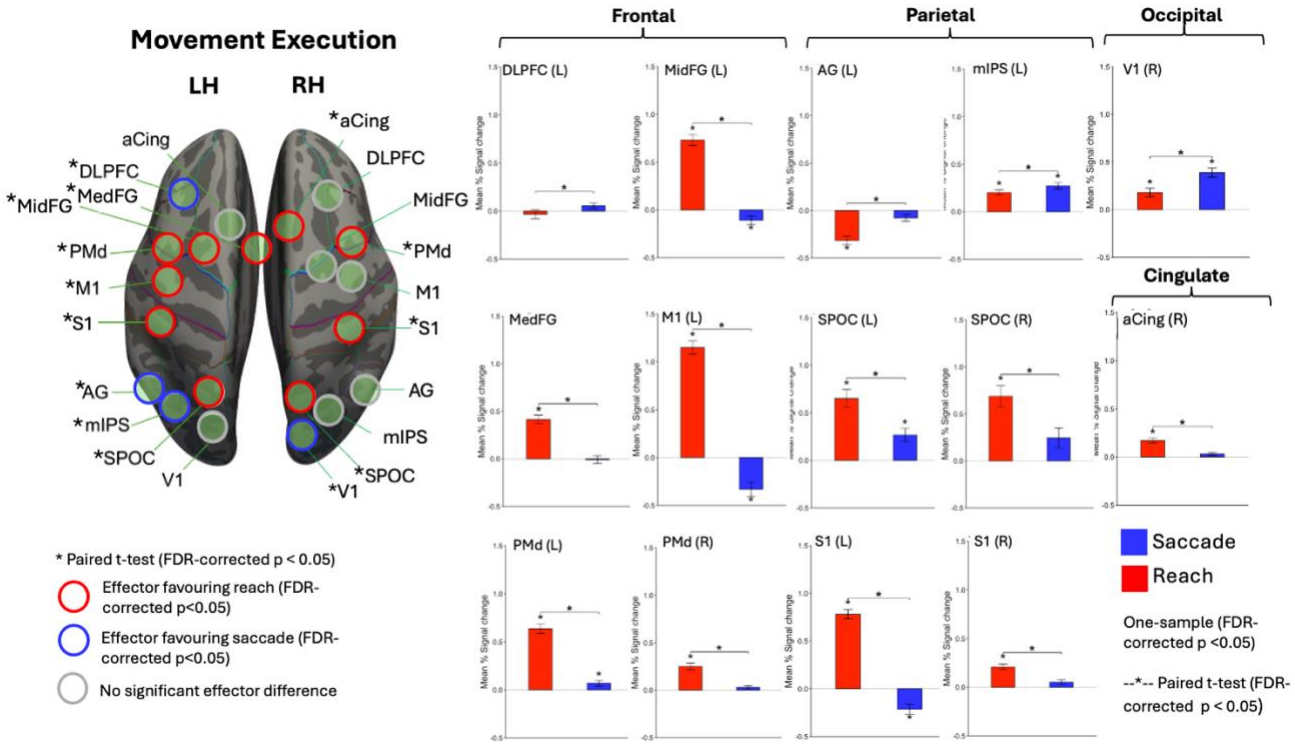


Figure 21: ROI analysis for selected regions during the movement execution phase. ROIs are displayed on the FreeSurfer fsaverage 'inflated' cortical surface (panel A). Asterisks beside ROI labels indicate a significant difference between the [Saccade>Colour] and [Reach>Colour] contrasts (paired *t*-test; FDR-corrected p<0,05). Red outlines identify ROIs with significantly greater mean % signal change values for reach compared to saccade, blue outlines identify ROIs with significantly greater mean % signal change for saccade compared to reach, and gray outlines represent no significant difference between effectors. Mean % signal change for ROIs showing a significant effector difference is plotted (panel B). Asterisks above bars indicate significant one-sample effects (FDR-corrected p<0.05), and brackets denote significant differences between effectors from paired t-tests (FDR-corrected p<0.05). Red bars correspond to reach values and blue bars to saccade. Error bars represent SEM.

CHAPTER 4: DISCUSSION

In this study, a cue-separated event-related fMRI paradigm was used to address three objectives. First, to characterize saccade and reach activity during effector-independent *visual target encoding*, as well as effector-dependent *movement planning* and *movement execution* phases. In the first phase, activity was limited to left middle frontal and temporal areas, while effector-dependent activity emerged during *movement planning*, with saccades recruiting posterior parietal regions and reaches engaging the broader occipital-parietal-frontal cortex. During *movement execution*, both saccade and reach network became strongly engaged along the cerebral cortex and cerebellum.

The second goal was to identify regions of overlapping activation during *movement planning* and *execution*. Common cortical activity was present within the same regions identified for the saccade network. Overlapping cerebellum activity was present but did not correspond to any peaks observed. Still, qualitative observations indicated overlap within the posterior bilateral lobules and the vermis.

The final objective was to identify saccade- and reach-preferential areas during *movement planning* and *movement execution*. During *movement planning*, saccade-preferential activity was observed in the ventral occipital cortex and cerebellum whereas reach-preferential activity was broad in dorsal occipital-parietal-frontal areas. During *movement execution*, saccades preferentially engaged occipital, lateral posterior parietal, superior and middle regions, as well as the cerebellum, while reaches preferentially showed peaks in left occipital-frontal areas, as well as the cerebellum. In an ROI analysis, we directly compared the magnitude of effect between saccades and reaches, particularly in brain regions typically studied in saccade and reach literature. We found greater activity for reaches compared to saccades during *movement planning* in bilateral DLPFC, MidFG, PMd, M1, SPOC, left AG, left mIPS, right aCing, and MedFG. During *movement execution*, saccade activity was greater in left mIPS and right V1, while reach activity was greater in bilateral PMd, SPOC, left MidFG, left M1, right aCing, and MedFG.

4.1 Effector versus colour activation across encoding, planning, and execution

4.1.1 Visual Target Encoding

During the *visual target encoding* phase, activity was observed within the left TP, left STG, and left MidFG. Activation of STG and MidFG is consistent with their established roles in spatial working memory (Geier et al., 2006) and spatial attention (Corbetta et al., 1998). MidFG, in particular, has been repeatedly implicated in the active maintenance of spatial location, though this lateralization is more commonly right-hemispheric (Owen et al., 1998; D'Esposito et al., 1998; Geier et al., 2006).

The left-lateralization of activity here be a result of participants preparing both reach and saccade responses before the action instruction. In that case, activity within these areas could be an early response for reach preparation with the right hand. In fact, Chen et al. (2014) similarly reported left MidFG activation during target encoding and their participants were aware of an upcoming required reach. The pattern of functional activity in these areas could also be related to the established left-lateralized network involved in language processing of action words (Boulenger et al., 2009). Thus, STG and MidFG activation likely reflect target location encoding, attention to a peripheral stimulus, early movement preparation, and language processing of the provided instructions.

The role of TP is less clear since this region is more associated with autobiographical memory and semantic-language processing, amongst other functions (Dupont, 2002). Its recruitment here may reflect its broader function as a multimodal convergence zone (Pascaul et al., 2015), supporting higher order integration of the spatial and contextual features of the target before upcoming movement.

4.1.2 Movement Planning

SACCADES. During saccade planning, activity was relatively limited, confined primarily to posterior parietal regions, including bilateral left SPL, and right PCu. There was also a small cluster within the left precentral gyrus. This pattern broadly agrees with previous studies isolating saccade planning activity (Astafiev et al., 2003; Beurze et al., 2009; Gallivan et al., 2011), although they reported more extensive frontal recruitment during this phase. The

restrained activation here is consistent with preliminary findings from Cappadocia et al. (2018) and supports the interpretation that the saccade network does not become fully engaged until closer to the time of execution.

REACHES. As hypothesized, reach planning produced broader activation spanning occipital, parietal, and frontal cortices with peaks in the left SPL, left SFG, and left FP. This distributed pattern aligns with established findings and likely reflects the more elaborate processing required within the frontal cortex for upper limb movements (Astafiev et al., 2003; Gorbet et al., 2004; Beruze et al., 2007; 2009; Gertz and Fiehler, 2015; Cappadocia et al., 2017). The differential patterns observed here for saccade versus reach highlight the importance of separating planning from encoding and execution stages of movement.

4.1.3 Movement Execution

SACCADES. During saccade execution, strong bilateral engagement emerged across the bilateral SPL, bilateral precentral gyrus, left Occipital Fus., left PCu, and left FP. This pattern aligns well with prior neuroimaging work (Astafiev et al., 2003; Koyama et al., 2004; Simo et al., 2005; Filimon et al., 2009). The recruitment of Occipital Fus. within the fusiform gyrus is notable, as this region is not typically reported in saccade studies, though its recruitment has been document (Corbetta et al., 1998). Its engagement here may reflect the reactivation of a visual memory for the target's location (Manelis et al., 2011). Alternatively, given the large extend of the cluster across much of the occipital cortex, activity here as a whole could represent visual processing as the eyes shift (Hagler et al., 2007; Levy et al., 2007).

REACHES. As hypothesized, reach execution produced broader cortical activation, with a left-lateralized distribution and peaks in the left postcentral gyrus and left precentral gyrus. These findings agree with the strong, contralateral somatosensory and primary motor involvement reported for reaching (Astafiev et al., 2003; Medendorp et al., 2005; Filimon et al., 2009; Cappadocia et al., 2017). While we did not observe any peaks within the well-characterizes regions of the posterior parietal and premotor cortices, the spatial pattern of our activation cluster confirmed the engagement of these regions. In addition, reach engaged the right lobule V, right lobule VIIIb, and vermis VIIIa of the cerebellum. The

ipsilateral engagement within these lobules is consistent with somatotropic maps of upper limb representation in the cerebellum (Grodd et al., 2001) and their engagement during reach tasks (Nitschke et al., 2004).

4.2 Overlapping Saccade and Reach activation

During *movement planning*, overlapping cortical activation for reach and saccades was confined to the same regions identified independently for saccade planning: bilateral SPL, right PCu, and left precentral gyrus. This pattern persisted into *movement execution*, where bilateral SPL and bilateral precentral gyrus, as well as the left PCu showed conjunctive activity. These findings agree with the hypothesis that shared overlap is present between these effectors and converges with a broad literature implicating the same parieto-frontal regions in both saccade and reach processing (Astafiev et al., 2003; Medendorp et al., 2005; Levy et al., 2007; Beurze et al., 2009; Filimon et al., 2009; Gallivan et al., 2011). The fact that shared activity was the same as the results found for saccade processing further confirms that reach and saccade recruit similar regions, with reaches engaging additional areas. Critically, the observed overlap here does not speak to the relative magnitude of activity for each effector, but it does offer an explanation for why dissociating effector-specific signals have proven to be difficult, especially when these networks are not directly contrasted with each other.

The shared role of spatial attention in these tasks must also be considered. It has been demonstrated that the saccade and spatial attention networks engage much of the same parieto-frontal regions (Corbetta et al., 1998; Astafiev et al., 2003). As both our reach and saccade conditions require spatial attention to remembered target location, our conjunction results may partly reflect the similar attentional demands required for both of these movements.

Overlapping activation was also identified in the cerebellum, encompassing hemispheric and vermal regions (including lobules VI, Crus I, and VIIIa, extending medially into vermis VI and VIIIa). Activity here did not coincide with peaks reported in either saccade or reach contrast independently. Still, this overlap is consistent with the established involvement of

these regions across separate saccade and reach execution tasks (Nitschke et al., 2004; Diedrichsen et al., 2005; Errante and Fogassi, 2020; Yamamoto et al., 2025). Thus, the present study suggests that these regions might play similar supporting roles in both effectors.

4.3 Effector-preferential activation across planning and execution

4.3.1 Movement Planning

SACCADES. Direct saccade and reach contrast during *movement planning* revealed limited saccade-preferential activity, with peaks in the bilateral Temporal Fus., right LOC, and left lobule I-IV in the cerebellum. The bilateral Temporal Fus. activation is unexpected given that this region is mostly associated with processes such as face recognition (Haxby et al., 1994), rather than oculomotor control. However, it may be involved spatial memory reactivation during saccade preparation (Manelis et al., 2011). More broadly, the lack of substantial dorsal occipital-parietal-frontal engagement is consistent with our hypothesis and previous findings showing exclusively reach-preferential activity during this phase (Cappadocia et al., 2018). This was also reinforced by ROI analyses, which revealed no regions, except the right mIPS, had saccade-related activity greater than the colour condition.

Saccade-related activity is typically observed in more posterior cerebellar regions (Nitschke et al., 2004; Simo et al., 2005; Yamamoto et al., 2005) while reach-related activity has been found in more anterior areas (Nitschke et al., 2004; Errante & Fogassi, 2020), which aligns with what we found during movement execution. Nevertheless, Alverez et al. (2010) reported increased activity for predictable versus random saccades within more anterior areas. Although target location was known for both effectors at this stage, activity in lobule I-IV may be related to the predictive processing of saccadic eye movements.

REACHES. In contrast, reach-preferential activity was broad, with peaks in the left SPL and left LOC. Moreover, the right aCing, bilateral DLPFC, MedFG, bilateral MidFG, bilateral PMd, bilateral M1, left AG, left mIPS, and bilateral SPOC all revealed significantly greater activity favoring this effector. These findings once again confirm that reach-planning activity is broader and stronger across the visuomotor network, at least earlier on during the

sensorimotor stages (Astafiev et al., 2003; Medendorp et al., 2005; Beurze et al., 2009; Cappadocia et al., 2018). Particularly for the PPC, previous studies have implicated the reach-specific role of SPOC in forming internal representations of spatial goals during reach planning (Fernandez-Ruiz et al., 2007), as well as mIPS and AG in integrating visual and proprioceptive information about hand position to form a reach vector (Vesia et al., 2010; Vesia and Crawford, 2012). Thus, our findings reflect the network involved in transforming sensory information into reach plans.

4.3.2 Movement Execution

SACCADES. The effector-preferential activity became most pronounced during *movement execution*. Saccade-preferential cortical engagement was observed across frontal, lateral posterior parietal, and occipital regions. Peaks were reported in the left Occipital Fus., left LG, left LOC, and left AG/SMG. ROI analyses revealed significantly greater saccade activity in left mIPS and right V1. Saccade preference within the occipital cortex is well-established (Hagler et al., 2007; Levy et al., 2007; Filimon et al., 2009) and can be attributed to the motion of the retinal image and visual input as the eyes shift fixations (Hagler et al., 2007; Levy et al., 2007; Filimon et al., 2009). Activation of AG and SMG during saccade tasks is well established (Simo et al., 2005; Schraa-Tam et al., 2009; Yamamoto et al., 2025), though whether these regions are preferentially active for saccades compared to reaches is less clear.

Previous fMRI work has shown reach-preference in AG (Filimon et al., 2009), while TMS evidence suggests this region plays a causal role in both reach and saccade movements (Vesia et al., 2010). Our cue-separated paradigm suggests that saccades preferentially activate these lateral PPC areas during movement execution. This would be consistent with the medial-lateral gradient that has been proposed along the IPS (Levy et al., 2007; Filimon et al., 2009) and extend this organization to the broader PPC. The greater activation for saccades in left mIPS also conflicts with previous reports of reach-preference (Filimon et al., 2009). During visuomotor preparation, left mIPS has been shown to decode spatial information rather than effector-type (Gallivan et al., 2011). The greater saccade activity in

mIPS during execution may therefore reflect the later spatial processing of the saccade network. Despite our hypothesis, there were no peaks in the posterior vermis, although a small cluster was observed with the left lobule VIIb, which is consistent with previous findings (Guillaume et al., 2018). The lack of preferential activity within the oculomotor vermis (VI-VII) could be due to arm movements also recruiting similar areas (Nitschke et al., 2004). Previous reports comparing eye versus hand tracking also led to no significant eye-related activation relative to hand movements (Miall et al., 2002).

REACHES. Reach-preferential activity was observed in the left postcentral gyrus and left LOC, as well as right lobule V and right lobule VIIIb. The ROI analysis revealed significantly greater reach-related activity in the right aCing, MedFG, left MidFG, bilateral PMd, left M1 and bilateral SPOC, which have been previously established (Astafiev et al., 2003; Filimon et al., 2009; Cappadocia et al., 2018). Reach-preferential activity in the left postcentral gyrus, as well as the activation extension into medial PPC regions, is consistent with our hypothesis (Levy et al., 2007; Filimon et al., 2009; Cappadocia et a., 2018), although the absence of peaks within discrete medial PPC areas precludes strong region-specific claims.

Finally, the reach-preferential peak in the right lobule V and right lobule VIIIb once again confirms the established cerebellar representation of upper limb movements in the anterior and posterior lobes (Grodd et al., 2001), further validating the activation of these areas in prior reach tasks (Nitschke et al., 2004; Errante and Fogassi, 2020). Since saccade and reach activity has not previously been directly contrasted in the same manner shown here, our findings might also newly indicate effector-specific roles of the right lobule V and lobule VIIIb in reach execution.

4.4 Limitations

The findings and interpretations of the present study might have been limited by several factors. First, our inability to clearly track the eye during the experiment does not allow us to directly confirm whether participants were fixating during the entire trial and shifting their gaze during saccade execution. However, our extensive training session, analysis of eye motion during Run 0, and online observation of the gaze during the experiment, provides us

with confirmation that participants were able to comply with the experimental demands. Equipment malfunctions during the scanning of four participants also prevented us from collecting behavioural data during these sessions. However, due to our training sessions and constant communication with participants during the experiment, we remain positive that participants performed the tasks correctly.

Furthermore, univariate analyses, although traditionally used in fMRI analyses, primarily detects differences in clusters of voxels and may miss finer-grained pattern differences within and between adjacent voxels. Using multivoxel pattern analysis (MVPA), Gallivan et al., (2011) was able to decode upcoming reach versus saccade preparatory activity even when signal amplitude differences were absent. However, we used an ROI analysis with constrained regions to attempt to isolate distinct differences that may not be captured using a cluster-based approach.

Many regions within the saccade and reach network overlap with parieto-frontal regions recruited for spatial attention (Astafiev et al., 2003). Although our control condition was designed to minimize general attentional contributions, some activity related to spatial attention may have contributed to the activity seen during the effector-dependent phases.

Lastly, in the present study, substantially more females than males were recruited due to generally greater interest from the female population in the local community for this experiment. As a result, we were unable to analyze the sex-based differences present in visually-guided actions. A previous study by Gorbet and Sergio (2007) that did look at sex-based differences found that females showed greater activation in premotor and parietal areas compared to males during reaching. It has also been established that males generally show larger activation volumes for upper limb tasks compared to females (Andrushko et al., 2023). We hypothesize that these effects would have been reflected in our results if we had equal numbers of female and male participants, and direct contrasts could have been performed.

4.5 Future Directions and Potential Applications

The findings of this study provide several important directions for future research. The observed overlap and effector-preferential activity within the cerebellum warrant further investigation. Future studies using higher resolution imaging procedures may help further distinguish functional specializations for saccade versus reach. For instance, Yamamoto et al. (2025) used a Human Connectome Project (HCP) protocol which lowered signal-to-noise ratio and found many more cerebellar regions activated for saccades compared to the present study. The findings of this study can also serve as a foundation for future functional and effector connectivity analyses that can examine the connections and directionality between saccade and reach preferential regions. Moreover, combining fMRI with causal approaches such as TMS can more accurately determine whether these areas are functionally necessary for saccade- and reach- processing, similar to the work conducted by Vesia et al. (2010).

This work has implications for clinical research surrounding rehabilitation of motor disorders. For example, lesions in the PPC, especially regions near and within SPL and IPS, can cause optic ataxia, in which reaches are impaired, despite the visual and motor system functioning normally (Perenin & Vighetto, 1988). This condition leaves voluntary eye movements largely unaffected, suggesting separate processing pathways for reaches and saccades within the PPC (Andersen et al., 2014). Characterizing effector-specific signals across the cortex will therefore inform the neuroanatomical framework required for rehabilitation efforts. This research also has the potential to contribute to brain-machine interfaces and prosthetic devices. Hauschild et al., (2012) showed that the macaque PRR and area 5d contain predictive reach-trajectory signals that can be decoded before movement execution. Thus, understanding the effector-specific modules within the PPC, especially for humans, can further inform the optimal locations for devices to record from.

4.6 Conclusion

Together, our findings confirm that temporally separated sensorimotor phases reveal differential temporal evolutions for saccade and reach, with characteristic cortical and

cerebellar activity at specific time points. We confirmed that there is overlapping activity along the bilateral parieto-frontal network during saccade and reach planning and execution, highlighting a reason for the difficulties present in detecting effector-specific dissociations without direct contrasts. When such contrasts were applied, a clearer picture emerged. During planning, saccade-preferential activity was minimal and confined to cerebellar and ventral regions, with the absence of dorsal parieto-frontal recruitment confirming the saccade network attains full engagement closer to execution. Conversely, reach-preferential planning activity was broadly present across the dorsal occipital-parietal regions. The most revealing findings appeared during the execution, where saccade-preferential activity in AG/SMG and reach-preferential activity extending to the medial PPC elaborates on the medial-lateral gradient previously proposed for these effectors. Additionally, reach-preferential activity within the ipsilateral cerebellum sheds light on non-cortical areas exhibiting stronger engagement for reaches relative to saccades. Our ROI analysis further revealed that during movement execution, many cortical regions show significantly greater activity for reach compared to saccade, with the exception of right V1 and left mIPS. These results confirm that effector-differential signals are present within the cortex and cerebellum, and they become most apparent when sensorimotor phases are separated in time.

REFERENCES

Alvarez, T. L., Alkan, Y., Gohel, S., Ward, B. D., & Biswal, B. B. (2010). Functional anatomy of predictive vergence and saccade eye movements in humans: A functional MRI investigation. *Vision Research, 50*(21), 2163–2175. https://doi.org/10.1016/j.visres.2010.08.018

Andersen, R. A., & Buneo, C. A. (2002). Intentional maps in posterior parietal cortex. Annual *Review of Neuroscience, 25*(1), 189–220. https://doi.org/10.1146/annurev.neuro.25.112701.142922

Andersen, R. A., Andersen, K. N., Hwang, E., & Hauschild, M. (2014). Optic ataxia: From Balint's syndrome to the parietal reach region. *Neuron, 81*(5), 967–983. https://doi.org/10.1016/j.neuron.2014.02.025

Andrushko, J. W., Rinat, S., Kirby, E. D., Dahlby, J., Ekstrand, C., & Boyd, L. A. (2023). Females exhibit smaller volumes of brain activation and lower inter-subject variability during motor tasks. *Scientific Reports, 13*, Article 17698. https://doi.org/10.1038/s41598-023-44889-x

Astafiev SV, Shulman GL, Stanley CM, Snyder AZ, Van Essen DC, & Corbetta M. (2003). Functional organization of human intraparietal and frontal cortex for attending, looking, and pointing. *The Journal of Neuroscience, 23*(11):4689-99. doi: 10.1523/JNEUROSCI.23-11-04689.2003

Bakola, S., Passarelli, L., Huynh, T., Impieri, D., Worthy, K. H., Fattori, P., Galletti, C., Burman, K. J., & Rosa, M. G. P. (2017). Cortical afferents and myeloarchitecture distinguish the medial intraparietal area (MIP) from neighboring subdivisions of the macaque cortex. *eNeuro, 4*(6), Article e0344-17.2017. https://doi.org/10.1523/ENEURO.0344-17.2017

Barash, S., Bracewell, R. M., Fogassi, L., Gnadt, J. W., & Andersen, R. A. (1991). Saccade-related activity in the lateral intraparietal area: I. Temporal properties; comparison with area 7a. *Journal of Neurophysiology*, *66*(3), 1095–1108.

Batista, A. P., Buneo, C. A., Snyder, L. H., & Andersen, R. A. (1999). Reach plans in eye-centered coordinates. *Science, 285*(5425), 257–260. https://doi.org/10.1126/science.285.5425.257

Beurze, S. M., de Lange, F. P., Toni, I., & Medendorp, W. P. (2007). Integration of target and effector information in the human brain during reach planning. *Journal of Neurophysiology, 97*(1), 188–199. https://doi.org/10.1152/jn.00456.2006

Beurze, S. M., de Lange, F. P., Toni, I., & Medendorp, W. P. (2009). Spatial and effector processing in the human parietofrontal network for reaches and saccades. *Journal of Neurophysiology, 101*(6), 3053–3062. https://doi.org/10.1152/jn.91194.2008

Blangero, A., Otac, H., Delporte, L., Revol, P., Vindras, P., Rode, G., Boisson, D., Vighetto, A., Rossetti, Y., & Pisella, L. (2007). Optic ataxia is not only "optic": Impaired spatial integration of proprioceptive information. *NeuroImage, 36*(1), T61–T68. https://doi.org/10.1016/j.neuroimage.2007.03.039

Blatt, G. J., Andersen, R. A., & Stoner, G. R. (1990). Visual receptive field organization and cortico-cortical connections of the lateral intraparietal area (area LIP) in the macaque. *Journal of Comparative Neurology, 299*(4), 421–445. doi: 10.1002/cne.902990404

Boulenger, V., Hauk, O., & Pulvermüller, F. (2009). Grasping ideas with the motor system: Semantic somatotopy in idiom comprehension. *Cerebral Cortex, 19*(8), 1905–1914. https://doi.org/10.1093/cercor/bhn217

Brodal, P. (1980). The projection from the nucleus reticularis tegmenti pontis to the cerebellum in the rhesus monkey. *Experimental Brain Research, 38*, 29–36. https://doi.org/10.1007/BF00237927

Bruce, C. J., & Goldberg, M. E. (1985). Primate frontal eye fields. I. Single neurons discharging before saccades. *Journal of Neurophysiology*, *53*(3), 603–635. https://doi.org/10.1152/jn.1985.53.3.603

Cameron, I. G. M., Riddle, J. M., & D'Esposito, M. (2015). Dissociable roles of dorsolateral prefrontal cortex and frontal eye fields during saccadic eye movements. *Frontiers in Human Neuroscience, 9*, 613. https://doi.org/10.3389/fnhum.2015.00613

Caminiti, R., Johnson, P. B., Galli, C., Ferraina, S., & Burnod, Y. (1991). Making arm movements within different parts of space: The premotor and motor cortical representation of a coordinate system for reaching to visual targets. *Journal of Neuroscience, 11*(5), 1182–1197. https://doi.org/10.1523/JNEUROSCI.11-05-01182.1991

Cappadocia, D. C., Monaco, S., Chen, Y., Blohm, G., & Crawford, J. D. (2017). Temporal evolution of target representation, movement direction planning, and reach execution in occipital-parietal-frontal cortex: An fMRI study. *Cerebral Cortex, 27*(11), 5242–5260. https://doi.org/10.1093/cercor/bhw304

Cappadocia, D. C., Monaco, S., Chen, Y., & Crawford, J. D. (2018). Cortical mechanisms for reaches versus saccades: Progression of effector-specificity through target memory to movement planning and execution [Preprint]. *bioRxiv*. https://doi.org/10.1101/415562

Chen, Y., Monaco, S., Byrne, P., Yan, X., Henriques, D.Y., & Crawford, J.D. (2014). Allocentric versus egocentric representation of remembered reach targets in human cortex. *The Journal of Neuroscience, 34(*37), 12515-26. doi: 10.1523/JNEUROSCI.1445-14.2014.

Chouinard, P. A., & Paus, T. (2006). The primary motor and premotor areas of the human cerebral cortex. *The Neuroscientist, 12*(2), 145–161. https://doi.org/10.1177/1073858405284255

Connolly, J. D., Andersen, R. A., & Goodale, M. A. (2003). fMRI evidence for a "parietal reach region" in the human brain. *Experimental Brain Research, 153*, 140–145. https://doi.org/10.1007/s00221-003-1587-5

Corbetta, M., Akbudak, E., Conturo, T. E., Snyder, A. Z., Ollinger, J. M., Drury, H. A., Linenweber, M. R., Petersen, S. E., Raichle, M. E., Essen, D. C. V., & Shulman, G. L. (1998). A common network of functional areas for attention and eye movements. *Neuron, 21*(4), 761–773. https://doi.org/10.1016/s0896-6273(00)80593-0

Crawford, J. D., Henriques, D. Y. P., & Medendorp, W. P. (2011). Three-dimensional transformations for goal-directed action. *Annual Review of Neuroscience, 34*, 309–331. https://doi.org/10.1146/annurev-neuro-061010-113749

Gorbet, D. J., & Sergio, L. E. (2007). Preliminary sex differences in human cortical BOLD fMRI activity during the preparation of increasingly complex visually guided movements. *European Journal of Neuroscience, 25*(4), 1228–1239. https://doi.org/10.1111/j.1460-9568.2007.05358.x

DeSouza, J. F. X., Menon, R. S., & Everling, S. (2003). Preparatory set associated with pro-saccades and anti-saccades in humans investigated with event-related fMRI. Journal of Neurophysiology, 89(2), 1016–1023. https://doi.org/10.1152/jn.00562.2002

D'Esposito, M., Aguirre, G. K., Zarahn, E., Ballard, D., Shin, R. K., & Lease, J. (1998). Functional MRI studies of spatial and nonspatial working memory. *Cognitive Brain Research, 7*(1), 1–13. https://doi.org/10.1016/S0926-6410(98)00004-4

Diedrichsen, J., Hashambhoy, Y., Rane, T., & Shadmehr, R. (2005). Neural correlates of reach errors. *Journal of Neuroscience, 25*(43), 9919–9931. https://doi.org/10.1523/JNEUROSCI.1874-05.2005

Dum, R. P., & Strick, P. L. (2003). An unfolded map of the cerebellar dentate nucleus and its projections to the cerebral cortex. *Journal of Neurophysiology, 89*(1), 634–639. https://doi.org/10.1152/jn.00626.2002

Dupont, S. (2002). Investigating temporal pole function by functional imaging. *Epileptic Disorders, 4*(Suppl. 1), S17–S22.

Errante, A., & Fogassi, L. (2020). Activation of cerebellum and basal ganglia during the observation and execution of manipulative actions. *Scientific Reports, 10*, 12008. https://doi.org/10.1038/s41598-020-68928-2

Esteban, O., et al. (2018). FMRIPrep: A robust preprocessing pipeline for functional MRI [Computer software]. Code Ocean. https://doi.org/10.24433/CO.ed5ddfef-76a3-4996-b298-e3200f69141b

Esteban, O., Markiewicz, C. J., Blair, R. W., Moodie, C. A., Isik, A. I., Erramuzpe, A., Kent, J. D., Goncalves, M., DuPre, E., Snyder, M., Oya, H., Ghosh, S. S., Wright, J., Durnez, J., Poldrack, R. A., & Gorgolewski, K. J. (2019). fMRIPrep: A robust preprocessing pipeline for functional MRI. *Nature Methods, 16*, 111–116. https://doi.org/10.1038/s41592-018-0235-4

Fernandez, L., Rogasch, N. C., Do, M., Clark, G., Major, B. P., Teo, W.-P., Byrne, L. K., & Enticott, P. G. (2020). Cerebral cortical activity following non-invasive cerebellar stimulation: A systematic review of combined TMS and EEG studies. *The Cerebellum, 19*(2), 309–335. https://doi.org/10.1007/s12311-019-01093-7

Fernandez-Ruiz, J., Goltz, H. C., DeSouza, J. F. X., Vilis, T., & Crawford, J. D. (2007). Human parietal "reach region" primarily encodes intrinsic visual direction, not extrinsic movement direction, in a visual–motor dissociation task. *Cerebral Cortex, 17*(10), 2283–2292. https://doi.org/10.1093/cercor/bhl137

Ferraina, S., Pare, M., & Wurtz, R. H. (2002). Comparison of cortico-cortical and cortico-collicular signals for the generation of saccadic eye movements. *Journal of Neurophysiology*, *87*(2), 845-858. doi: 10.1152/jn.00317.2001

Filimon, F., Nelson, J. D., Huang, R.-S., & Sereno, M. I. (2009). Multiple parietal reach regions in humans: Cortical representations for visual and proprioceptive feedback during on-line reaching. Journal of Neuroscience, 29(9), 2961–2971. doi: 10.1523/JNEUROSCI.3211-08.2009

Fisch, L., Zumdick, S., Barkhau, C., Emden, D., Ernsting, J., Leenings, R., Sarink, K., Winter, N. R., Risse, B., Dannlowski, U., & Hahn, T. (2024). deepbet: Fast brain extraction of T1-weighted MRI using convolutional neural networks. *Computers in Biology and Medicine, 179*, 108845. https://doi.org/10.1016/j.compbiomed.2024.108845

Fu, Q.-G., Flament, D., Coltz, J. D., & Ebner, T. J. (1997). Relationship of cerebellar Purkinje cell simple spike discharge to movement kinematics in the monkey. *Journal of Neurophysiology, 78*(1), 478–491. https://doi.org/10.1152/jn.1997.78.1.478

Fujikado, T., & Noda, H. (1987). Saccadic eye movements evoked by microstimulation of lobule VII of the cerebellar vermis of macaque monkeys. The Journal of Physiology, 394(1), 573–594. doi: 10.1113/jphysiol.1987.sp016885

Funahashi, S., Bruce, C. J., & Goldman-Rakic, P. S. (1989). Mnemonic coding of visual space in the monkey's dorsolateral prefrontal cortex. *Journal of Neurophysiology, 61*(2), 331–349. doi: 10.1152/jn.1989.61.2.331

Gallivan, J. P., McLean, D. A., Smith, F. W., & Culham, J. C. (2011). Decoding effector-dependent and effector-independent movement intentions from human parieto-frontal brain activity. *Journal of Neuroscience, 31*(47), 17149–17168. https://doi.org/10.1523/JNEUROSCI.1058-11.2011

Galletti, C., & Battaglini, P. P. (1989). Gaze-dependent visual neurons in area V3A of monkey prestriate cortex. *The Journal of Neuroscience, 9*(4), 1112–1125. doi: 10.1523/JNEUROSCI.09-04-01112.1989

Galletti, C., Fattori, P., Kutz, D. F., & Battaglini, P. P. (1997). Arm movement-related neurons in the visual area V6A of the macaque superior parietal lobule. *European Journal of Neuroscience, 9*(2), 410-413. https://doi.org/10.1111/j.1460-9568.1997.tb01410.x

Geier, C. F., Garver, K. E., & Luna, B. (2006). Circuitry underlying temporally extended spatial working memory. *NeuroImage, 35*(2), 904–915. https://doi.org/10.1016/j.neuroimage.2006.12.022

Gertz, H., & Fiehler, K. (2015). Human posterior parietal cortex encodes the movement goal in a pro-/anti-reach task. *Journal of Neurophysiology, 114*(1), 170-183. https://doi.org/10.1152/jn.01039.2014

Gorbet, D. J., Staines, W. R., & Sergio, L. E. (2004). Brain mechanisms for preparing increasingly complex sensory to motor transformations. *NeuroImage, 23*(3), 1100–1111. https://doi.org/10.1016/j.neuroimage.2004.07.043

Grodd, W., Hülsmann, E., Lotze, M., Wildgruber, D., & Erb, M. (2001). Sensorimotor mapping of the human cerebellum: fMRI evidence of somatotopic organization. *Human Brain Mapping, 13*(2), 55–73. https://doi.org/10.1002/hbm.1025

Guillaume, A., Fuller, J. R., Srimal, R., & Curtis, C. E. (2018). Cortico-cerebellar network involved in saccade adaptation. *Journal of Neurophysiology, 120*(5), 2583–2594. https://doi.org/10.1152/jn.00392.2018

Hagler, D. J., Jr., Riecke, L., & Sereno, M. I. (2007). Parietal and superior frontal visuospatial maps activated by pointing and saccades. NeuroImage, 35(4), 1562–1577. https://doi.org/10.1016/j.neuroimage.2007.01.033

M. Hauschild,G.H. Mulliken,I. Fineman,G.E. Loeb, & R.A. Andersen, Cognitive signals for brain–machine interfaces in posterior parietal cortex include continuous 3D trajectory commands, *Proceedings of the National Academy of Sciences*. *109*(42), 17075-17080, https://doi.org/10.1073/pnas.1215092109 (2012).

Haxby, J. V., Horwitz, B., Ungerleider, L. G., Maisog, J. M., Pietrini, P., & Grady, C. L. (1994). The functional organization of human extrastriate cortex: A PET-rCBF study of selective attention to faces and locations. Journal of Neuroscience, 14(11), 6336–6353. https://doi.org/10.1523/JNEUROSCI.14-11-06336.1994

Hewitt, A. L., Popa, L. S., & Ebner, T. J. (2015). Changes in Purkinje cell simple spike encoding of reach kinematics during adaption to a mechanical perturbation. *The Journal of Neuroscience, 35*(3), 1106–1124. https://doi.org/10.1523/JNEUROSCI.2579-14.2015

Hikosaka, O., Sakamoto, M., & Miyashita, N. (1993). Effects of caudate nucleus stimulation on substantia nigra cell activity in monkey. *Experimental Brain Research, 95*, 457–472. https://doi.org/10.1007/BF00227139

Hoover, J. E., & Strick, P. L. (1999). The organization of cerebellar and basal ganglia outputs to primary motor cortex as revealed by retrograde transneuronal transport of herpes simplex virus type 1. *The Journal of Neuroscience, 19*(4), 1446–1463. https://doi.org/10.1523/JNEUROSCI.19-04-01446.1999

Inomata-Terada, S., Fukuda, H., Tokushige, S., Matsuda, S.-i., Hamada, M., Ugawa, Y., Tsuji, S., & Terao, Y. (2023). Abnormal saccade profiles in hereditary spinocerebellar degeneration reveal cerebellar contribution to visually guided saccades. *Clinical Neurophysiology, 154*, 70–84. https://doi.org/10.1016/j.clinph.2023.07.006

Izawa, J., Criscimagna-Hemminger, S. E., & Shadmehr, R. (2012). Cerebellar contributions to reach adaptation and learning sensory consequences of action. *The Journal of Neuroscience, 32*(12), 4230–4239. https://doi.org/10.1523/JNEUROSCI.6353-11.2012

Jamadar SD, Fielding, J., & Egan, G.F. (2013). Quantitative meta-analysis of fMRI and PET studies reveals consistent activation in fronto-striatal-parietal regions and cerebellum during antisaccades and prosaccades. *Frontiers in Psychology, 4*(749). doi: 10.3389/fpsyg.2013.00749

Jenkinson, M., Beckmann, C. F., Behrens, T. E. J., Woolrich, M. W., & Smith, S. M. (2012). FSL. *NeuroImage, 62*(2), 782–790. https://doi.org/10.1016/j.neuroimage.2011.09.015

Johnson, P. B., Ferraina, S., Bianchi, L., & Caminiti, R. (1996). Cortical networks for visual reaching: Physiological and anatomical organization of frontal and parietal lobe arm regions. *Cerebral Cortex, 6*(2), 102–119. https://doi.org/10.1093/cercor/6.2.102

Kakei, S., Hoffman, D. S., & Strick, P. L. (1999). Muscle and movement representations in the primary motor cortex. *Science, 285*(5436), 2136–2139. https://doi.org/10.1126/science.285.5436.2136

Kalaska, J. F., & Crammond, D. J. (1992). Cerebral cortical mechanisms of reaching movements. *Science, 255*(5051), 1517–1523. https://doi.org/10.1126/science.1549781

Kapoula, Z., Yang, Q., Coubard, O., Daunys, G., & Orssaud, C. (2005). Role of the posterior parietal cortex in the initiation of saccades and vergence: Right/left functional asymmetry. *Annals of the New York Academy of Sciences, 1039*(1), 184–197. doi: 10.1196/annals.1325.018

Kelly, R. M., & Strick, P. L. (2003). Cerebellar loops with motor cortex and prefrontal cortex of a nonhuman primate. *The Journal of Neuroscience, 23*(23), 8432–8444. https://doi.org/10.1523/JNEUROSCI.23-23-08432.2003

Koyama, M., Hasegawa, I., Osada, T., Adachi, Y., Nakahara, K., & Miyashita, Y. (2004). Functional magnetic resonance imaging of macaque monkeys performing visually guided saccade tasks: Comparison of cortical eye fields with humans. Neuron, 41(5), 795-807. doi: 10.1016/s0896-6273(04)00047-9

Künzle, H., & Akert, K. (1977). Efferent connections of cortical area 8 (frontal eye field) in Macaca fascicularis: A reinvestigation using the autoradiographic technique. Journal of Comparative Neurology, 173(1), 147–164. doi: 10.1002/cne.901730108

Levy, I., Schluppeck, D., Heeger, D. J., & Glimcher, P. W. (2007). Specificity of human cortical areas for reaches and saccades. *The Journal of Neuroscience, 27*(17), 4687-4696. https://doi.org/10.1523/JNEUROSCI.0459-07.2007

Manelis, A., Hanson, C., & Hanson, S. J. (2011). Implicit memory for object locations depends on reactivation of encoding-related brain regions. *Human Brain Mapping, 32*(1), 32–50. https://doi.org/10.1002/hbm.20992

Mayka, M. A., Corcos, D. M., Leurgans, S. E., & Vaillancourt, D. E. (2006). Three-dimensional locations and boundaries of motor and premotor cortices as defined by functional brain imaging: A meta-analysis. *NeuroImage, 31*(4), 1453–1474. https://doi.org/10.1016/j.neuroimage.2006.02.004

Medendorp, W. P., Goltz, H. C., Vilis, T., & Crawford, J. D. (2003). Gaze-centered updating of visual space in human parietal cortex. *The Journal of Neuroscience, 23*(15), 6209–6214. https://doi.org/10.1523/JNEUROSCI.23-15-06209.2003

Medendorp, W. P., Goltz, H. C., Crawford, J. D., & Vilis, T. (2005). Integration of target and effector information in human posterior parietal cortex for the planning of action. *Journal of Neurophysiology, 93*(2), 954–962. https://doi.org/10.1152/jn.00725.2004

Miall, R. C., Imamizu, H., & Miyauchi, S. (2000). Activation of the cerebellum in co-ordinated eye and hand tracking movements: An fMRI study. *Experimental Brain Research, 135*(1), 22–33. https://doi.org/10.1007/s002210000491

Nitschke, M. F., Arp, T., Stavrou, G., Erdmann, C., & Heide, W. (2004). The cerebellum in the cerebro-cerebellar network for the control of eye and hand movements—An fMRI study. *Progress in Brain Research, 148*, 151–164. https://doi.org/10.1016/S0079-6123(04)48013-3

Nitschke, M. F., Binkofski, F., Buccino, G., Posse, S., Erdmann, C., Kompf, D., Seitz, R. J., & Heide, W. (2004). Activation of cerebellar hemispheres in spatial memorization of saccadic eye movements: An fMRI study. Human Brain Mapping, 22(2), 155-164. doi: 10.1002/hbm.20025

Noda, H., Sugita, S., & Ikeda, Y. (1990). Afferent and efferent connections of the oculomotor region of the fastigial nucleus in the macaque monkey. *Journal of Comparative Neurology, 302*(2), 330–348. doi: 10.1002/cne.903020211

Ohtsuka, K., & Noda, H. (1991). Saccadic burst neurons in the oculomotor region of the fastigial nucleus of macaque monkeys. *Journal of Neurophysiology, 65*(6), 1422–1434. doi: 10.1152/jn.1991.65.6.1422

Owen, A. M., Stern, C. E., Look, R. B., Tracey, I., Rosen, B. R., & Petrides, M. (1998). Functional organization of spatial and nonspatial working memory processing within the human lateral frontal cortex. *Proceedings of the National Academy of Sciences of the United States of America, 95*(13), 7721–7726. https://doi.org/10.1073/pnas.95.13.7721

Pascual, B., Masdeu, J. C., Hollenbeck, M., Makris, N., Insausti, R., Ding, S.-L., & Dickerson, B. C. (2015). Large-scale brain networks of the human left temporal pole: A functional connectivity MRI study. *Cerebral Cortex, 25*(3), 680–702. https://doi.org/10.1093/cercor/bht260

Perenin, M.-T., & Vighetto, A. (1988). Optic ataxia: A specific disruption in visuomotor mechanisms. I. Different aspects of the deficit in reaching for objects. *Brain, 111*(3), 643–674. https://doi.org/10.1093/brain/111.3.643

Popa, L. S., Hewitt, A. L., & Ebner, T. J. (2012). Predictive and feedback performance errors are signaled in the simple spike discharge of individual Purkinje cells. *The Journal of Neuroscience, 32*(44), 15345–15358. https://doi.org/10.1523/JNEUROSCI.2151-12.2012

Pouget, P. (2015). The cortex is in overall control of "voluntary" eye movement. *Eye, 29*(2), 241–245. https://doi.org/10.1038/eye.2014.284

Rayner, K. (1998). Eye movements in reading and information processing: 20 years of research. *Psychological Bulletin, 124*(3), 372–422. https://doi.org/10.1037/0033-2909.124.3.372

Robinson, D. A. (1972). Eye movements evoked by collicular stimulation in the alert monkey. *Vision Research*, *12*(11), 1795–1808. https://doi.org/10.1016/0042-6989(72)90070-3

Rolls, E.Rolls, E. T., Deco, G., Huang, C.-C., & Feng, J. (2023). The human posterior parietal cortex: effective connectome, and its relation to function. Cerebral Cortex, 33(6), 3142–3170. https://doi.org/10.1093/cercor/bhac266

Sartin, S., Ranzini, M., Scarpazza, C., & Monaco, S. (2023). Cortical areas involved in grasping and reaching actions with and without visual information: An ALE meta-analysis of neuroimaging studies. *Current Research in Neurobiology, 4*, 100070. https://doi.org/10.1016/j.crneur.2022.100070

Schall, J. D., & Hanes, D. P. (1993). Neural basis of saccade target selection in frontal eye field during visual search. *Nature, 366*(6454), 467–469. https://doi.org/10.1038/366467a0

Schlag, J., & Schlag-Rey, M. (1987). Evidence for a supplementary eye field. Journal of Neurophysiology, 57(1), 179–200. doi: 10.1152/jn.1987.57.1.179

Schraa-Tam, C. K. L., van Broekhoven, P., van der Geest, J. N., Frens, M. A., Smits, M., & van der Lugt, A. (2009). Cortical and cerebellar activation induced by reflexive and voluntary saccades. *Experimental Brain Research, 192*, 175-187. https://doi.org/10.1007/s00221-008-1569-4

Sereno, M. I., Pitzalis, S., & Martinez, A. (2001). Mapping of contralateral space in retinotopic coordinates by a parietal cortical area in humans. *Science, 294*(5545), 1350–1354. https://doi.org/10.1126/science.1063695

Simó, L. S., Krisky, C. M., & Sweeney, J. A. (2005). Functional neuroanatomy of anticipatory behavior: Dissociation between sensory-driven and memory-driven systems. *Cerebral Cortex, 15*(12), 1982–1991. https://doi.org/10.1093/cercor/bhi073

Smith, S. M., & Nichols, T. E. (2009). Threshold-free cluster enhancement: Addressing problems of smoothing, threshold dependence and localisation in cluster inference. *NeuroImage, 44*(1), 83–98. https://doi.org/10.1016/j.neuroimage.2008.03.061

Snyder, L. H., Batista, A. P., & Andersen, R. A. (1997). *Coding of intention in the posterior parietal cortex*. *Nature*, 386(6621), 167–170. https://doi.org/10.1038/386167a0

SR Research Ltd. (2025, September 25). EyeLink 1000 Plus technical specifications. https://www.sr-research.com/eyelink-1000-plus-technical-specifications/

Stanton, G. B., Goldberg, M. E., & Bruce, C. J. (1988). Frontal eye field efferents in the macaque monkey: II. Topography of terminal fields in midbrain and pons. *Journal of Comparative Neurology, 271*(4), 493–506. https://doi.org/10.1002/cne.902710403

Trillenberg, P., Sprenger, A., Petersen, D., Kömpf, D., Heide, W., & Helmchen, C. (2007). Functional dissociation of saccade and hand reaching control with bilateral lesions of the medial wall of the intraparietal sulcus: Implications for optic ataxia. *NeuroImage, 36*(Supplement 2), T69–T76. https://doi.org/10.1016/j.neuroimage.2007.03.038

Vesia, M., & Crawford, J. D. (2012). Specialization of reach function in human posterior parietal cortex. *Experimental Brain Research, 221*, 1–18. https://doi.org/10.1007/s00221-012-3149-1

Vesia, M., Prime, S. L., Yan, X., Sergio, L. E., & Crawford, J. D. (2010). Specificity of human parietal saccade and reach regions during transcranial magnetic stimulation. The *Journal of Neuroscience, 30*(39), 13053–13065. https://doi.org/10.1523/JNEUROSCI.1644-10.2010

Vesia, M., Yan, X., Henriques, D. Y., Sergio, L. E., & Crawford, J. D. (2008). Transcranial magnetic stimulation over human dorsal–lateral posterior parietal cortex disrupts integration of hand position signals into the reach plan. *Journal of Neurophysiology, 100*(4), 2005–2014. https://doi.org/10.1152/jn.90519.2008

Vingerhoets, G. (2014). Contribution of the posterior parietal cortex in reaching, grasping, and using objects and tools. *Frontiers in Psychology, 5*, 151. https://doi.org/10.3389/fpsyg.2014.00151

Wang, N., Perkins, E., Zhou, L., Warren, S., & May, P. J. (2013). Anatomical evidence that the superior colliculus controls saccades through central mesencephalic reticular formation gating of omnipause neuron activity. *Journal of Neuroscience, 33*(41), 16285–16296. https://doi.org/10.1523/JNEUROSCI.2726-11.2013

Weinrich, M., & Wise, S. P. (1982). The premotor cortex of the monkey. *Journal of Neuroscience, 2*(9), 1329–1345. https://doi.org/10.1523/JNEUROSCI.02-09-01329.1982

Winkler, A. M., Ridgway, G. R., Webster, M. A., Smith, S. M., & Nichols, T. E. (2014). Permutation inference for the general linear model. *NeuroImage, 92*, 381–397. https://doi.org/10.1016/j.neuroimage.2014.01.060

Woolrich, M. W., Ripley, B. D., Brady, M., & Smith, S. M. (2001). Temporal autocorrelation in univariate linear modeling of FMRI data. *NeuroImage, 14*(6), 1370–1386. https://doi.org/10.1006/nimg.2001.0931

Wu, J., Ngo, G. H., Greve, D., Li, J., He, T., Fischl, B., Eickhoff, S. B., & Yeo, B. T. T. (2018). Accurate nonlinear mapping between MNI volumetric and FreeSurfer surface coordinate systems. *Human Brain Mapping, 39*(9), 3793–3808. https://doi.org/10.1002/hbm.24213

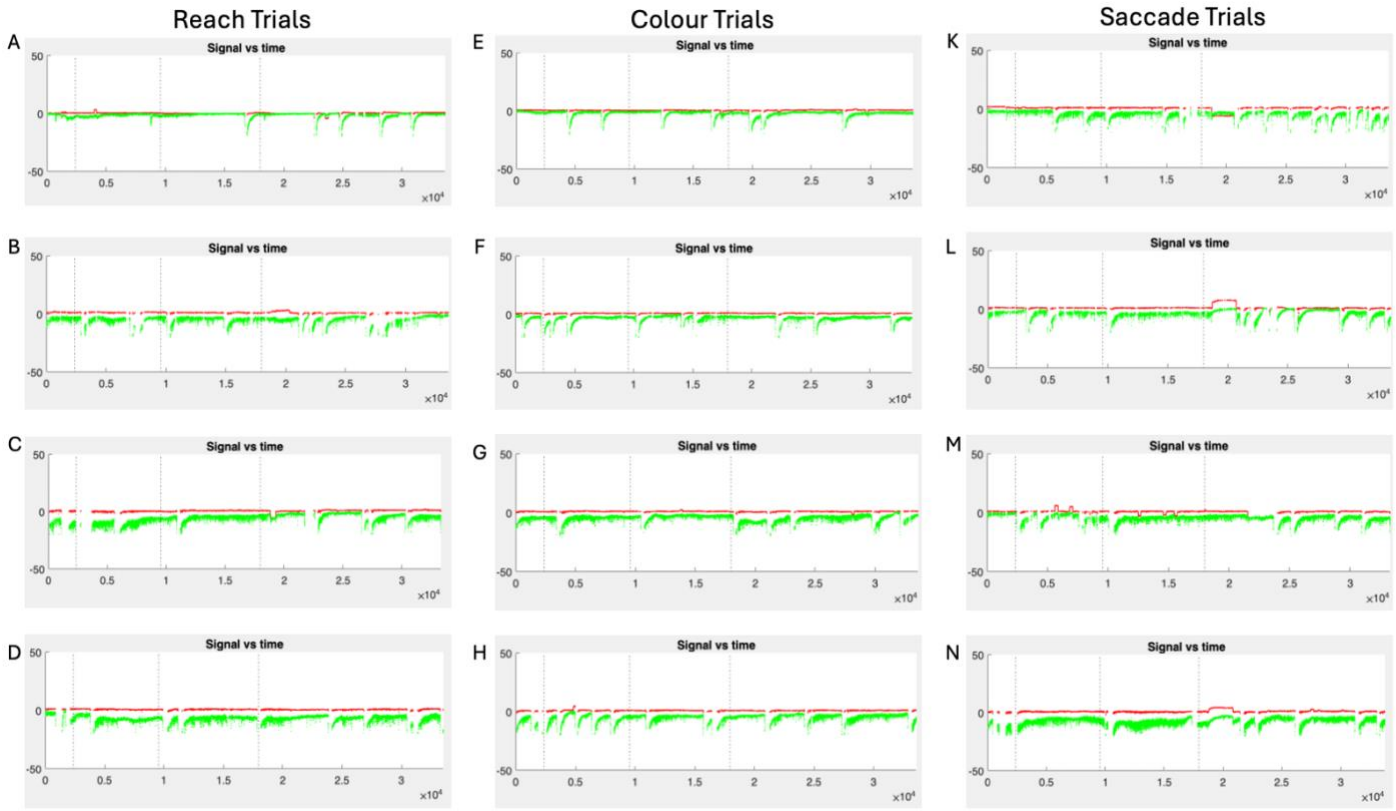
Yamamoto, T., Miura, K., Matsuda, K., Matsumoto, J., Hashimoto, R., Ono, S., Sadato, N., & Fukunaga, M. (2025). Brain-wide activation and deactivation maps during smooth and saccadic tracking in humans. Cerebral Cortex, 35(8), Article bhaf242. https://doi.org/10.1093/cercor/bhaf242

Yang, Q., & Kapoula, Z. (2011). Distinct control of initiation and metrics of memory-guided saccades and vergence by the FEF: A TMS study. *PLoS ONE, 6*(5), e20322. https://doi.org/10.1371/journal.pone.0020322

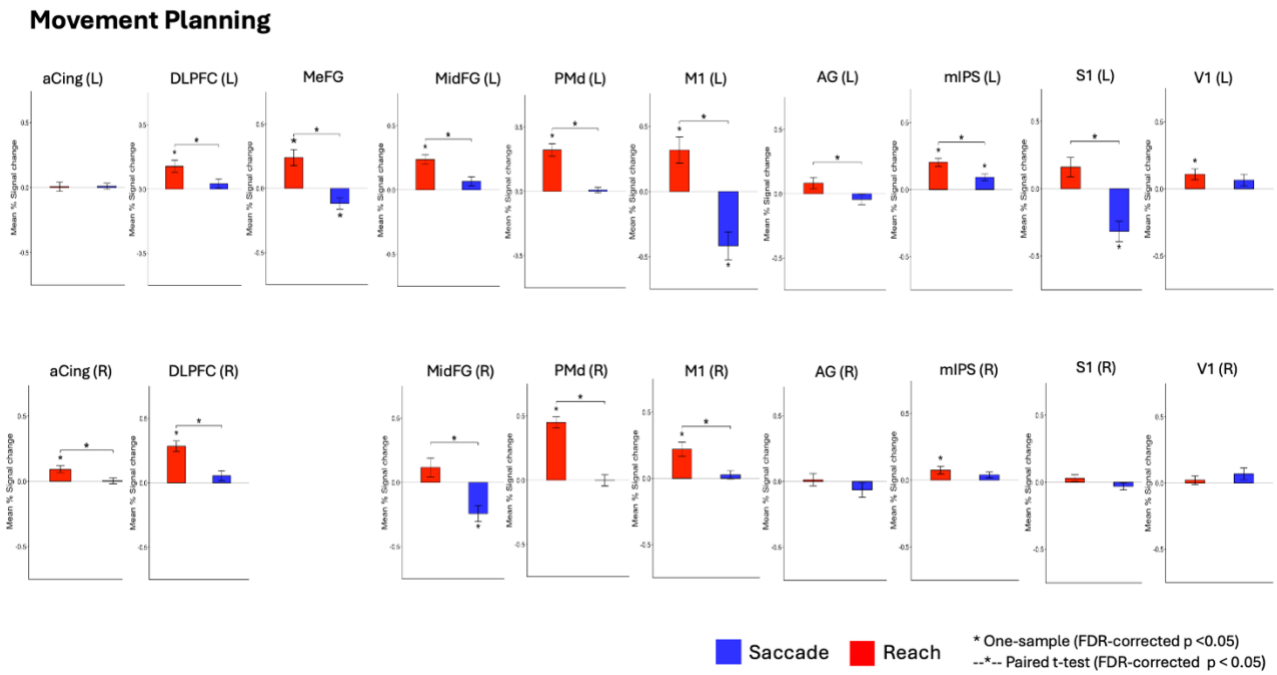
APPENDIX

Appendix A: Trial information (condition and target direction), target colour, and behavioural information recorded using an in-house custom MATLAB program across all trials for a representative participant (sub19) during Run 0. In the Button Press column, a value of 1 indicates that button presses were recorded for the trial, with the parentheses indicating how many times the button was pressed. In the Reach column, a value of 1 indicates that a reach response was recorded. In the Reach Error column, a value of 1 indicates that a directional error occurred during the recorded reach response (e.g., target was presented to the left of the central fixation point, but the reach was recorded to the right). Trials are shown in the same order presented to the participant during Run 0.

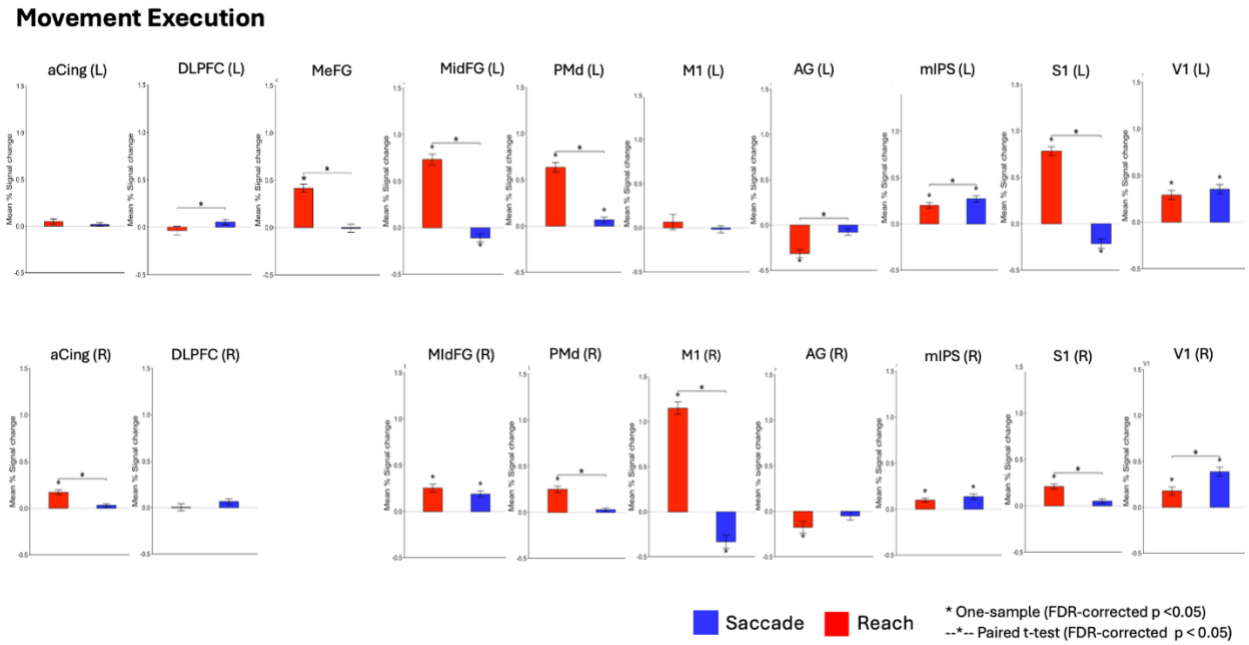
Trial Information	**Target Colour**	**Button Press (1=yes; 0=no)**	**Reach (1=yes; 0 = no)**	**Reach Error (1=yes; 0=no)**
Reach – Left	Red	0	1	0
Colour – Left	Green	1 (once)	0	
Colour – Right	Green	1 (once)	0	
Saccade – Left	Red	0	0	
Saccade – Right	Green	0	0	
Reach – Right	Red	0	1	0
Saccade – Left	Green	0	0	
Colour – Left	Red	1 (twice)	0	
Colour – Right	Red	1 (twice)	0	
Reach – Right	Green	0	1	0
Reach – Left	Green	0	1	0
Saccade – Right	Red	0	0	



Appendix B: Eye position over time (seconds) across all trials for a representative participant (sub19) during Run 0. Signal-vs-time plots show horizontal (red) and vertical (green) gaze positions across individual trials. Vertical dotted lines indicated the onset of the visual target encoding, movement planning, and movement execution phases. Gaze data was calibrated using the participant-specific calibration procedure, with eye position represented in degrees of visual angle relative to the calibrated central fixation LED location (0°, 0°). Flat gaze traces indicate periods of stable fixation, whereas deviations in the traces reflect horizontal and vertical eye movements. Rightward eye movements are represented by upward shifts in the horizontal gaze trace (red), whereas leftward eye movement are represented by downward shifts. A – D correspond to the reach condition and E – H correspond to the colour condition, during which participants were instructed to maintain fixation throughout the trial. Trials K – N correspond to the saccade condition, in which participants were required to shift their gaze during the movement execution phase in the following directions: K – left; L – right; M – left; N – right.



Appendix C: Mean % signal change for all ROIs during the movement planning phase. Asterisks above bars indicate significant one-sample effects (FDR-corrected $p<0.05$), and brackets denote significant differences between effectors from paired t-tests (FDR-corrected $p<0.05$). Red bars correspond to reach values and blue bars to saccade. Error bars represent SEM.



Appendix D: Mean % signal change for all ROIs during the movement execution phase. Asterisks above bars indicate significant one-sample effects (FDR-corrected $p<0.05$), and brackets denote significant differences between effectors from paired t-tests (FDR-corrected $p<0.05$). Red bars correspond to reach values and blue bars to saccade. Error bars represent SEM.